REPORT DOCUMENTATION PAGE

Form Approved OMB No. 0704-0188

1. REPORT DATE (DD-MM-YYYY) 16-04-2008	2. REPORT TYPE Final Report	3. DATES COVERED (From – To) 26-Feb-07 - 22-May-08

4. TITLE AND SUBTITLE

Characterization and Optimization of Vacuum-arc Plasma Generator for Nanocomposite Tribological Coating Growth

5a. CONTRACT NUMBER
STCU Registration No: P-251

5b. GRANT NUMBER

5c. PROGRAM ELEMENT NUMBER

6. AUTHOR(S)

Dr. Volodymyr Evgenievich Strelnytskiy

5d. PROJECT NUMBER

5d. TASK NUMBER

5e. WORK UNIT NUMBER

7. PERFORMING ORGANIZATION NAME(S) AND ADDRESS(ES)
Kharkov Institute of Physics and Technology
Akademicheskaya Str.1
Kharkov 61108
Ukraine

8. PERFORMING ORGANIZATION REPORT NUMBER

N/A

9. SPONSORING/MONITORING AGENCY NAME(S) AND ADDRESS(ES)

EOARD
Unit 4515 BOX 14
APO AE 09421

10. SPONSOR/MONITOR'S ACRONYM(S)

11. SPONSOR/MONITOR'S REPORT NUMBER(S)
STCU 06-8004

12. DISTRIBUTION/AVAILABILITY STATEMENT

Approved for public release; distribution is unlimited.

13. SUPPLEMENTARY NOTES

14. ABSTRACT

This report results from a contract tasking Kharkov Institute of Physics and Technology as follows: Development of new plasma deposition methods is critical for nanocomposite and nanostructured material growth. For example, to address the issues of ambient/space cycling, high-temperature lubrication, and reliability of space and air vehicles, new advanced coatings were developed by AFRL which need a combination of ceramic matrices and solid lubricant inclusions. This research project is directed to develop and optimize power supply for filtered vacuum arc generator located at AFRL/MLBT to enable the production of such unique composite coatings. In particular, the new power unit will provide a stable plasma filtering and delivery into synthesis chamber under conditions of strong magnetic fields for dielectric material growth. The commercially available technology is not capable of such task, due to a lack of understanding and control of the power supply current-voltage characteristics for non-metallic ionic current and density distributions in the arc plasma. This research project will tap the unique expertise of Ukrainian scientists in filtered vacuum arc technology, which was invented in Dr. Strelnitskiy's group. AFRL is currently evaluating the technology benefits for various tribological applications in both air and space vehicles. The new development suggested by this project will expand the range of materials to include insulating ceramic matrices, such as AL_2O_3 and ZrO_2, for preparation of nanocomposite and nanostructured tribological coatings. This will provide a new capability for AFRL research in advanced wear and friction reducing coatings for aerospace. The project includes transfer of the research results, developed equipment, and technological procedures for the use in AFRL/MLBT research and development programs.

15. SUBJECT TERMS
EOARD, Materials, Coatings, Colorants and Finishes

16. SECURITY CLASSIFICATION OF:			17. LIMITATION OF ABSTRACT UL	18, NUMBER OF PAGES	19a. NAME OF RESPONSIBLE PERSON WYNN SANDERS, Maj, USAF
a. REPORT UNCLAS	b. ABSTRACT UNCLAS	c. THIS PAGE UNCLAS		38	19b. TELEPHONE NUMBER (Include area code) +44 (0)1895 616 007

Standard Form 298 (Rev. 8/98)
Prescribed by ANSI Std. Z39-18

FINAL REPORT
Performing Period: 03/01/07 – 02/29/08

Subcontract No. P-251

Characterization and optimization of vacuum-arc plasma generator for nanocomposite tribological coating growth

National Science Centre
Kharkov Institute of Physics and Technology

List of figures

1. Summary

At the First Stage of the Project the research on stability of the vacuum-arc plasma source provided with a conventional DC power supply with ballast resistor (SBR) was carried out. The experimental results were obtained in various modes of the source operation. Research was done using the existing laboratory facilities. The scheme and design of the main units of the switching power supply source (SPS, or PSS) and the SPS as a whole was developed.

At the Second Stage of the Project the experimental version of the switching power supply (SPS) was manufactured and tested.

At the Third Stage of the Project the research on operation of the vacuum-arc plasma source provided with experimental version of the SPS and optimization of its characteristics was made. Comparison of the performance of the vacuum-arc plasma source supplied with SPS and SBR was carried out. Final version of the SPS was manufactured. Power value of 6 kW and the upper limit output current value of 120A were reached in final version of the SPS.

At the Fourth Stage of the Project the final version of the SPS was tested when operating with the vacuum-arc plasma source in the regimes of dielectric coating deposition.

2. Introduction

Two main tasks were solving during the Project: optimization of vacuum-arc plasma generator and development the switching power supply suitable for nanocomposite tribological coating growth. Vacuum-arc plasma generator used for coatings deposition includes a vacuum-arc plasma source and a power supply.

An important characteristic of a vacuum-arc plasma source is stability of its operation in various modes specified by requirements of technological processes such as deposition of nano-structural wear-resistant coatings. Stability of the arc discharge is usually characterized by frequency of spontaneous arc breaking [1]. It is necessary to note, that stability of an arc burning is determined by both parameters of the power supply (power reserve, open-circuit voltage, inductance and capacity of an external circuit) and the technological parameters of deposition processes (pressure and kind of the working gas; arc current; material of the cathode; magnitude and configuration of magnetic field; resistance of the coatings deposited on electrodes of the device). At the First Stage of the Project the results of research on stability of the vacuum-arc plasma source provided with a conventional DC power supply with ballast resistor (BR) were obtained. The experimental results were obtained in various modes of the source operation.

Power supply is one of the main parts of the vacuum-arc plasma generator. It is necessary maintain the proper arc current, arc voltage, stable regime of the source operation during the process of coatings deposition. Arc voltage drop is of 30-40 V for such commonly used cathode materials as Ti, Al. But when the dielectric coatings are deposited, the arc voltage is increased to 50-60 V. General purpose supplies are not able operate at so high voltage level. That's why it was necessary to develop specialized power supply suitable for vacuum-arc plasma facility.

DC power supplies with a ballast resistor (SBR) generally used in laboratory and industry practice have satisfactory characteristics for a feed of vacuum-arc plasma sources, however they are characterized by increased power losses in BR, large dimensions and weight.

In contrast with SBR the switching power supply exhibits efficiencies of between 70 to 90 percent, regardless of the input voltage, because the switching regulator of the power devices operates in the full-on and cutoff states, and so power losses are small [2].

In the world market there are a plenty of switched power supplies (SPS) for an arc feeding, having considerably smaller dimensions and weight [3]. Such power supplies are not needed in BR. However, all of them are intended for welding works at atmospheric pressure and do not provide stability of vacuum arc because of fast fluctuations of arc current and high voltage drop on the arc discharge.

The purpose of the present Project is development of the scheme of the switched power supply for feeding a vacuum-arc plasma source which is suitable for deposition of nano-structural non-conducting composite coatings. The principle of pulse-width modulation (PWM) is used in the scheme as more expedient.

For estimation the suitability of the power supply developed it was necessary to compare performance of the vacuum-arc plasma source provided with such power supply and that of conventional one, commonly used in industrial vacuum-arc installations. Comparison of the performance of the vacuum-arc plasma source supplied with SPS and SBR was carried out at the Third Stage of the Project. Vacuum-arc discharge characteristics were measured in the regimes of deposition of conductive Al and non-conductive (dielectric) AlN coatings. Stability of the vacuum-arc plasma source operation was investigated. Frequency of casual arc breaking was measured. Power transferred from the SPS into the arc discharge was measured in various modes of the source operation.

3. Methods, assumptions and procedures

3.1 Experimental details of research on arc stability at deposition of conducting and non-conducting AlN coatings

Research on performance of the vacuum-arc plasma source provided with a conventional DC power supply with ballast resistor (BR) was carried out using the existing laboratory facilities. In Fig. 1 the schematic drawing of installation for coatings deposition with use of a filtered vacuum-arc plasma source is presented.

The installation contains the vacuum chamber 1 with pumping-out system (not shown in the drawing), filtered vacuum-arc plasma source (FVAPS) 2, including consumable cathode 3 placed in the case 4, stabilizing magnetic coil 5, the cylindrical anode 6 electrically isolated from the case 4, curvilinear plasma-guide 7 with input 8,9, output 10 and deflecting 11, 12 magnetic coils, power supplies of magnetic coils (they are not shown in the drawing), arc power supply 13 with an adjustable ballast resistor (BR) 14, ampere-meters for measuring of an arc current I_c 15 and anode current I_a 16, working gas feeding system 17 containing the adjustable valve 18 for feeding plasma source with Ar from the vessel 19 and the controllable valve 20 for introducing N_2 gas into the
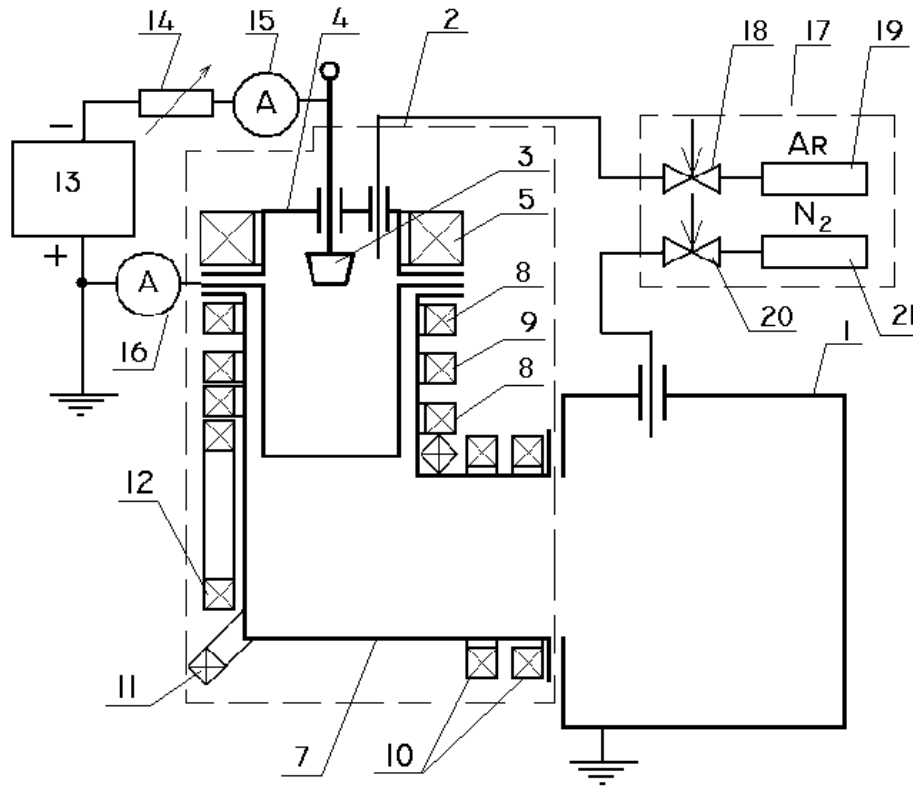
Fig.1. Schematic drawing of installation for coatings deposition.

vacuum chamber from the vessel 21. The controllable valve 20 is driven by the system of automatic maintenance of set pressure of the working gas (not shown in the drawing). The magnitude and configuration of the magnetic field inside the cylindrical anode 6 could be adjusted varying magnitude and direction of a current in the coil 9.

Aluminium was chosen as a material of the cathode that allowed deposition both metal Al, and dielectric AlN coatings.

Following parameters were varied during Al and AlN coatings deposition and finding the ranges of plasma source stable operation:

− pressure of Ar (at Al coatings deposition) P_{Ar} ;

− arc current I_c;

− argon gas concentration C_{Ar} in (Ar+N_2) mix (at AlN coatings deposition);

− magnitude and direction of the current I_9 in the coil 9 (see Fig.1), determining the magnetic field magnitude and configuration inside the anode (the currents in all the rest magnetic coils of the plasma source are fixed).

For increase the stability of the vacuum-arc source operation at deposition of AlN coatings the working gas components were introduced separately: Ar gas was injected near to the cathode of the plasma source, and N_2 gas – directly in the vacuum chamber.

During investigation of the plasma source operation the following parameters were measured in various modes:

− arc voltage drop U_a;

5

− anode current I_a at the fixed total arc current I_c;

− frequency of arc breaking **f**.

Separate measurement of the anode current I_a and the total current of the discharge I_c is caused by the presence of the magnetic field in the filter. Thus the electronic current flows through two parallel circuits: from the cathode to the anode across a magnetic field lines and from the cathode to the grounded chamber along the magnetic field lines. As the anode is located near to the cathode, just the anode current plays a defining role in stability of the arc discharge. Varying the magnitude and configuration of the magnetic field in the anode it is possible to adjust currents flowing through these two circuits and so influence stability of an arc burning.

For deposition of dielectric AlN coatings $Ar+N_2$ mix was used as the working gas. As a rule, at filtered vacuum-arc AlN coatings deposition the mix pressure $P_{Ar+N2} \approx 3 \cdot 10^{-3}$ Torr was sustained. The choice of the working mix pressure is motivated by two reasons. On the one hand, at higher pressure the output ion current of the filter decreases. At smaller pressure the quality of AlN coatings worsens. Experiments were carried out at two fixed arc current values. The first one, $I_c =55$ A is chosen from condition of minimization of emission of macro-particles from the Al cathode and stable burning of the arc. The second one, $I_c = 90$ A is an average arc current value commonly used in vacuum-arc deposition processes.

3.2 Development of the scheme of the switching power supply (SPS). Comparison with SBR (Supply with Ballast Resistor)

Usual power supply with linear regulator operates by reducing a higher input voltage down to the lower output voltage linearly controlling the conductivity of a series pass power device (a ballast resistor (BR)) in response to changes in its load. As a result large voltage drop V_{drop} across the BR with the load current I_{load} flowing through it arises. This *headroom loss* ($V_{drop} \cdot I_{load}$) causes the linear regulator to be only 30 to 50 percent efficient.

The switching regulator of the power devices operates in the full-on and cutoff states. As a result either large current being passed through the power devices with a low "on" voltage or no current flowing with high voltage across the device. Consequently power losses within the supply are small. The average switching power supply exhibits efficiencies of between 70 to 90 percent, regardless of the input voltage.

Using pulse switching power supplies (SPS) is more preferable for a feed of the vacuum-arc plasma sources in comparison with usual low-frequency ones due to their following advantages.

1. High coefficient of efficiency (up to 90 %).

2. The compact dimensions.

3. High efficiency and accuracy of an output current and voltage regulation.

4. Availability the appropriate semiconductor power components considerably simplifies design of the SPS.

There is a set of schemes of the SPS. However for output power values from kilowatt and higher it is more expedient to use the bridge scheme represented in Fig. 2.
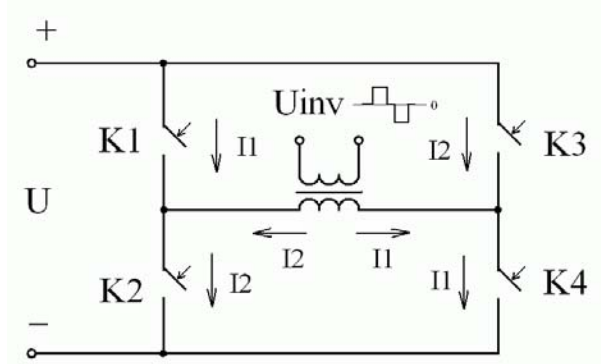
Fig. 2. Bridge scheme of the SPS.
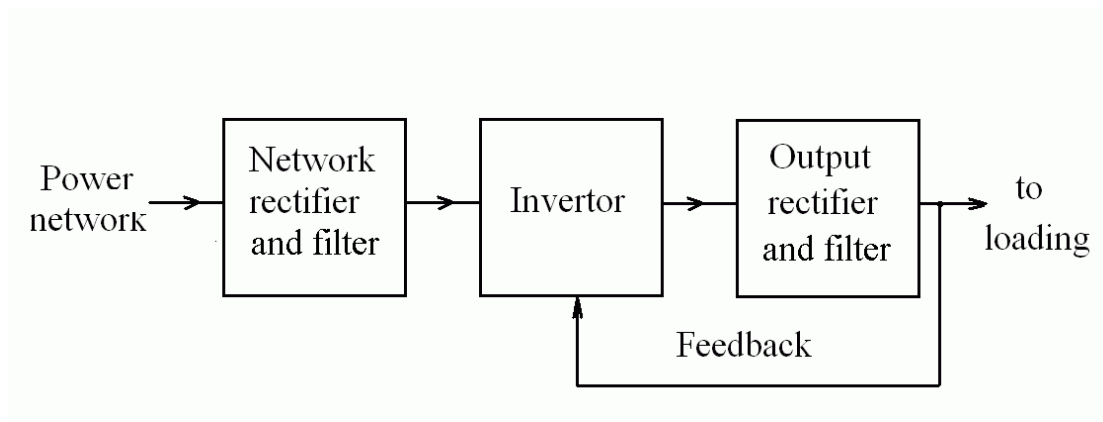
Fig. 3. Block diagram of the SPS.

Principle of operation of such power supply is following (see Fig. 3).

The AC current of a network comes in the network rectifier with the filter where it is rectified and filtered, and then comes in the inverter.

The SPS (see Fig. 2) will transform DC voltage U in AC one with peak value U_{inv}. Under influence of an external control signal the pairs of semiconductor series power switches К1, К4 and then К2, К3 are alternately switched on and off. There are two distinct time periods which occur when the switches are on and off, t_{on} and t_{off} accordingly. The resistance of switches in the state 'on' is negligible quantity. So when the pair К1, К4 turns on, the input voltage U is placed directly across the primary winding of the transformer and drives the current I_1 in it. Similarly at switching "on" the pair К2, К3, current I_2 equals to I_1, but opposite in direction, flows in the winding. Thus, on the secondary winding there appears voltage U_{inv} with peak values "+U·k" and " - U·k ", where k is a turn ratio

$$k=W_2/W_1,$$

where W_1 is number of turns of a primary transformer winding, W_2 is number of turns of a secondary one.

From an output of the inverter the voltage U_{inv} comes in the output rectifier with the filter where it is rectified and filtered.

Thus, on the SPS output there will appear DC output voltage of magnitude U_{out}:

7

$$U_{out} = k \cdot U \cdot D, \qquad\qquad (1)$$

where D is the duty cycle ($D = t_{on}/(t_{on} + t_{off})$).

Apparently from the formula an output voltage of the power supply (at U = constant) depends only on the duty cycle value:

$$D = t_{on}/T = t_{on} \cdot f , \qquad\qquad (2)$$

where t_{on} - duration of the switches "on" state, T, f - repetition period and frequency of U_{inv} accordingly.

The t_{on} value can be varied within the limits from 0 up to (T - t_{off}) where $t_{off} = 2 \cdot t_d$ - time interval along which all switches of the inverter are "off". Presence t_d (so called "dead time") in the formula for D is connected with finite value of the time commutating of the semi-conductor switches. Therefore in order to prevent occurrence of a through current in real inverter schemes the "dead time" is taken into account. For the majority of power switches t_d is in the range of 1 - 5 μsec. From expressions 1 and 2 it is visible that adjustment of U_{out} value is possible in two ways: varying t_{on} or f. The first way in power electronics is called pulse-width modulation (PWM), and the second one is pulse-frequency modulation (PFM).

Optimized variant of regulation depends on the working frequency. From the past experience of designing of powerful pulse sources the lower limit of the frequency is 20 kHz. This lower value is determined first of all by dimensions of transformers and inductor coils. This value is increased inversely to working frequency of the SPS. The upper value we shall set is of 50 kHz. It is limited first of all by performance of power switches. So for regulation of a current and a voltage over a wide range it is more expedient to use PWM.

It is known, that duration of transient phenomena in a vacuum arc, caused by spontaneous variations of an arc voltage drop and arc current, is less than 1 μsec. Time of reaction of the designed power supply even at the maximal frequency 50 kHz cannot be less than 40-60 μsec. It is connected with the peculiarity of the feedback scheme. 2-3 cycles of switching of the inverter are needed for generating proper feedback voltage.

In this connection for improving the transient performance of the power supply loaded with a vacuum arc and shaping the falling volt-ampere (V-A) load characteristic the additional ballast inductor coil is included in series with the primary winding of the pulse transformer.

Estimation of the V-A characteristic of the power supply with a ballast inductor coil was made on base of an equivalent circuit shown in Fig. 4.
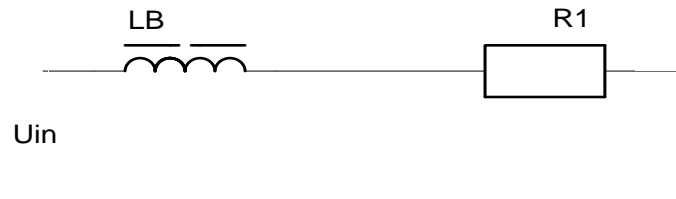
Fig.4. Equivalent circuit of the power supply with a ballast inductor coil.

L_b - ballast inductor coil; R_1 - active load resistance reduced to a primary circuit.

For estimation the output V-A characteristic of the power supply we shall take into account well known expression:

$$I = \frac{U}{\sqrt{x_L^2 + R_1^2}},\qquad\qquad (3)$$

where U is input variable voltage, X_L is inductive impedance of the ballast inductor coil at the working frequency, R_1 is the active load resistance reduced to a primary circuit: $R_1 = R_2 \cdot \left(\frac{1}{k}\right)^2$, where R_2 is the active resistance of load (arc), k is turn ratio.

Substituting in the formulas the load resistor value (estimated from the arc current) and considering that $U_2 = U_1 \cdot k$, and $I_2 = I/k$, we can estimate the load characteristic of the power supply. It is plotted as the curve 1 in Fig. 5.
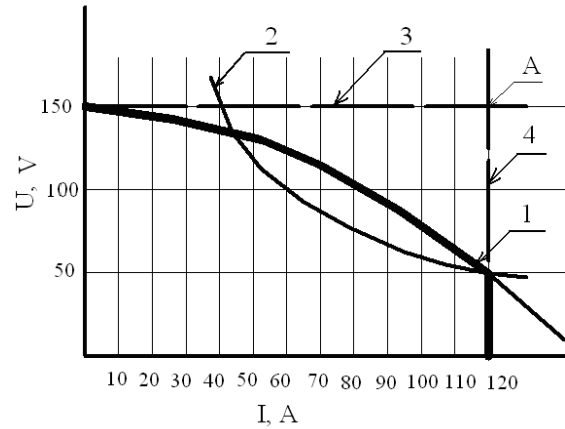
Fig.5. Estimated characteristic of the SPS.
1 – SPS load V-A characteristic; 2 - curve of constant power (6 kW); 3 - line of the maximal output voltage; 4 - line of the maximal output current.

As shown in Fig.5, without use of the ballast inductor coil the load V-A characteristic of the power supply having two regulators (a voltage and a current) looks like a rectangle, limited by lines of the maximal output voltage (a straight line 3) and the maximal output current (a straight line 4). It is easy to see, that without use of the ballast inductor coil the maximal output power will be 18 kW, that is three times exceeds the chosen nominal output power of the designed power supply. Therefore at long-duration SPS operation outside the region of ultimate load it will be either disconnected due to overheat, or destroyed.

From the performance of the power switch transistors used in the scheme designed, and considering that switching of transistors occurs in a "rigid" mode, the working frequency is chosen nearby 27 kHz. Accordingly, the inductance of a ballast inductor coil should be of 20 μH. For X_L calculated at the first harmonic of working frequency the falling shape of the load V-A characteristic will be realized (curve 1 in Fig. 5).

From Fig.5 it is clear, that the load characteristic of the source has falling shape with a vertical line 4 at current value of 120 A. From the curve 1 it is clear that the maximal output

power of a source in this case does not exceed 8 kW that is admissible overload of the power supply. At adjustment of the output current to be lower than its maximal value, vertically falling part of the load characteristic (a straight line 3) will be displaced to the left.

3.3 The description of the SPS scheme and the power supply operation

3.3.1 Basic elements of the scheme and their destination

Block diagram of the SPS is shown in Fig. 6.
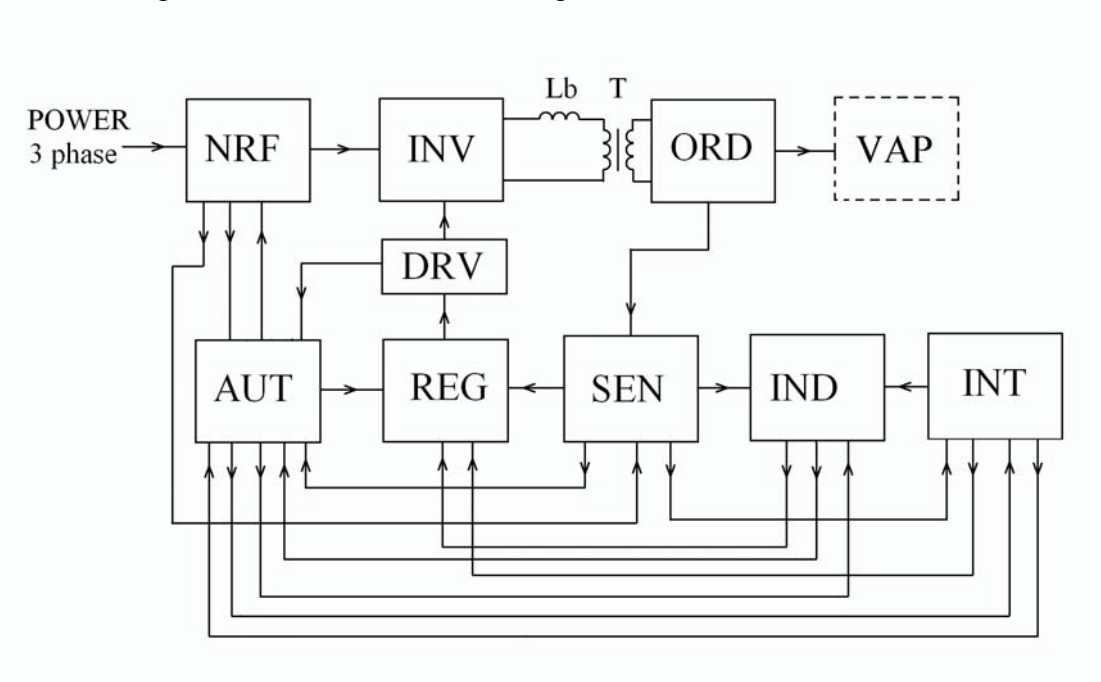
Fig. 6. Block diagram of the SPS. NRF - network rectifier with filter; INV - inverter; ORD - output rectifier with an inductor coil; VAP - vacuum-arc plasma source; AUT - module of automatics; REG - PWM regulator module; DRV - drivers; SEN - module of measuring instruments; IND - module of control and indication; INT - interface of remote control; L_b - ballast inductor coil; T - the pulse transformer.

NRF contains: bridge rectifier, inductor coil of the network filter, filtering capacitors, starting three-phase relay, charging resistor, relay for shunting the charging resistor.

Inverter INV contains: IGBT transistors (switches), snubber being placed across the primary winding of the transformer and snubber capacitors intended for protection of transistors from over-voltage.

ORD contains diodes of the output rectifier and an output inductor coil.

The AUT module consists of circuit plate of automatics, thermal relay and current transformer. The circuit plate of automatics provides:

1. Turning on the starting relay, turning on the relay, which shunts the charging resistor with 3-4 sec delay after turning on the starting relay.
2. Turning on the PWM regulator module with 3-4 sec delay after shunting of charging resistor.

3. Emergency shutdown of the SPS in case an overheating of power transistors and diodes or excess of an admissible current through a primary winding of transformer T.
4. Data transfer on control panel IND for mapping and on interface module INT.

The module of measuring instruments (SEN) consists of the current-sensing device, voltage-sensing device, voltmeter for measuring voltage on capacitors of the NRF module and amplifiers for voltage reduction for modules REG, IND and INT.

Module SEN provides:
1. Measurement of the load current and voltage for mapping those on the control panel and for use in modules REG, IND and INT of the power supply.
2. Measurement of the voltage on NRF capacitors, comparison it with permissible limit and generation the signal on emergency shutdown of a power unit in case of over-voltage.

All measuring instruments are electrically isolated from the power circuits of the SPS.

Module REG consists of the clock generator which sets clock rate (working frequency) of PWM and INV operation. PWM itself consists of amplifiers of the voltage and current "mistakes", generator of voltage of saw-tooth waveform, and comparator. The comparator compares a voltage of saw-tooth waveform with an output voltage of amplifiers of "mistake" and on the base of comparison the module forms proper duration of PWM pulses. From an output of the comparator these pulses come in the scheme which generates para-phase pulses for control of the switches of the bridge inverter.

The module of control and indication IND consists of the digital voltmeter and the ampere-meter for displaying the voltage and the current magnitude on the control panel.

The control panel contains the control buttons "START", "STOP" and "RESET", the switch "SETUP-WORK", a potentiometer for regulation of an output current and the indicating light-emitting diodes (LEDs), glow of which represents the current status of the power supply.

Except for the modules represented on the block diagram there is a module of service power supply consisting of the power supply generating a DC voltage for a feed of AUT and REG modules, and the generator of a "meander"-shaped voltage with frequency of 40-70 kHz. "Meander" provides electrically isolated feed of DRV and SEN modules.

3.3.2 Description of the power supply operation

At turn on the SPS, an AC network voltage comes in the service power supply (not shown). Thus the DC feed voltage comes in all cardboards of AUT, REG, DRV, SEN, IND modules, and the green LED „POWER SPS" and digital LED indicators begin glow. After that the required value of the output current can be adjusted by regulator "I" at position "SETUP" of the switch "SETUP-WORK".

After pressing "START" button the three-phase relay operates and AC network voltage comes in the rectifier bridge. The capacitors of the network filter are charging with rectified current flowing through the charging resistor. After 3-4 sec delay the relay for shunting the charging resistor operates. Then after further 2-3 sec delay the PWM scheme becomes operate, and duration of pulses which control the drivers of four semi-conductor switches K1-K4 of inverter INV becomes gradually increase.

In case of failure of one or several power transistors, the cardboard of drivers AUT module generates the signal on switching-off the three-phase relay and switching-off the feed of a network rectifier. At the same time the red LED "ERROR" on the control panel becomes glow.

At normal mode of operation of power transistors the inverter starts to generate AC voltage which is rectified and filtered and comes in the output of the SPS. Open-circuit voltage

of the SPS is of 150 V. This value is displayed on digital indicator "VOLTAGE". In this case PWM scheme generates the control pulses of maximal duration.

At operation with the load (vacuum-arc source) PWM scheme adjusts proper pulses duration ensuring the maintenance of pre-set arc current value in the range of V-A characteristic. The value of the pre-set arc current is displayed on the digital indicator "CURRENT" at position "WORK" of the switch "SETUP-WORK".

4. Results and discussion

4.1.   Research on the arc stability at deposition of conducting Al coatings (SBR supply)

Fig. 7 (a,b) shows the dependence of an arc voltage drop U_a and an anode current I_a on pressure of gas (argon) for the fixed arc current $I_c = 55$ A at two values of current in coil 9 (I_9).

a)

b)
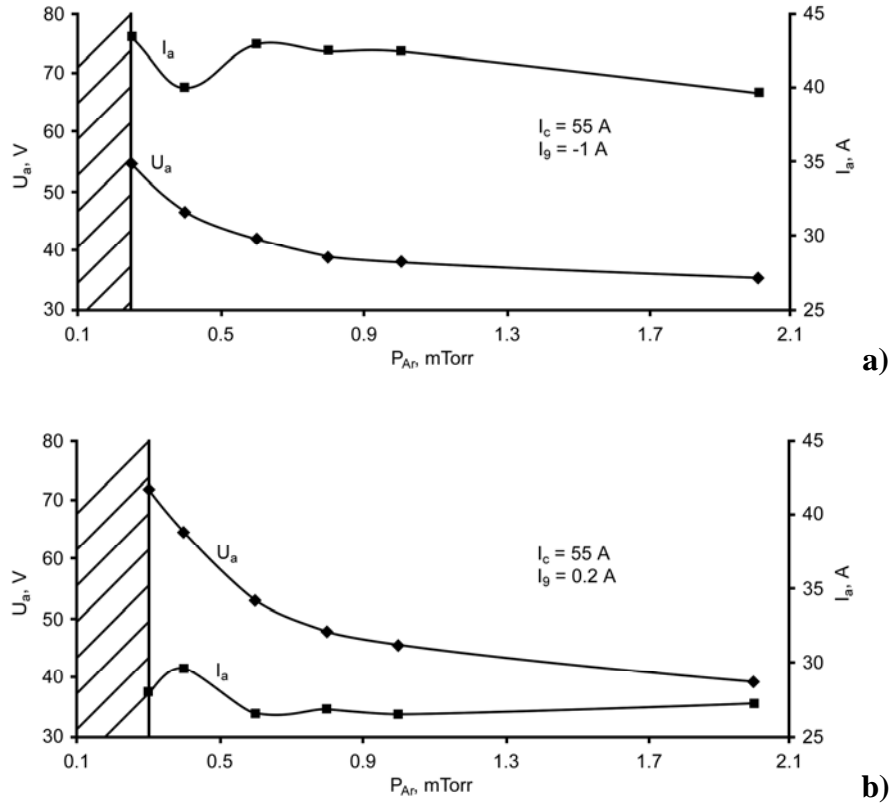
Fig.7. Arc voltage drop U_a and anode current I_a versus argon gas pressure. I_c=55 A.

Negative value of current I_9 in the coil corresponds to its opposite energizing with respect to currents in other magnetic coils of a plasma source. During experiments the arc was initiated at Ar pressure of $2 \cdot 10^{-3}$ Torr. Then Ar pressure was gradually decreasing till the moment of arc breaking. The shaded area on plots Figs.7, 8 corresponds to pressure range at which the arc can not be initiated.

Fig. 8 (a,b) shows similar dependences for I_c =90 A.
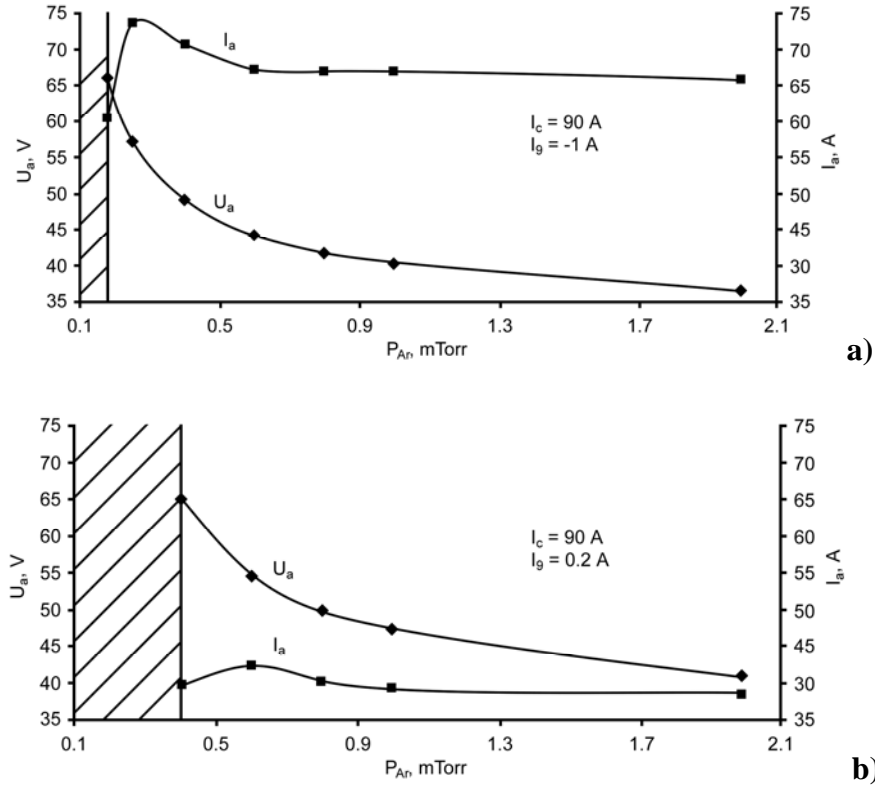
Fig.8. Arc voltage drop U_a and anode current I_a versus argon gas pressure. I_c=90 A.

Experimental points on curves Figs. 7, 8 correspond to the range of pressure at which the arc burns stably. At lower values of P_{Ar} the arc was extinguished and could not be initiated. Fig. 7 reveals that decrease of Ar pressure from 1.7 mTorr down to 0.2 mTorr results in increase of the arc voltage drop from 27 V up to 55 V, respectively ($I_c = 55$ A, $I_9 = -1$ A). The anode current varies slightly. Similar dependence is observed also for $I_9 = 0.2$ A.

It is worth to be noted, that in all experimental conditions the arc voltage drop at which the arc extinguishes is approximately equals to $55 \div 65$ V. It is connected with the fact that the open-circuit voltage of the arc power supply is not sufficient for maintaining predetermined magnitude of the arc current. To improve vacuum-arc stability it is necessary to increase open-circuit voltage of the power supply. However it will require increase of BR resistance that will be resulted in increase of losses of energy.

Variations of the magnetic field inside the anode (by varying the current I_9 in coil 9) causes more essential changes of the arc voltage drop U_a and the anode current I_a.

Fig. 9 shows typical dependence of the arc voltage drop U_a and the anode current I_a on current I_9 in the anode coil 9.

Fig.9. Arc voltage drop U_a and anode current I_a as functions of current I_9 in the coil 9.

Apparently from Fig.9 that the greater is the magnetic field inside the anode the greater is the arc voltage drop U_a and smaller the anode current I_a at the fixed arc current. Increase of the magnetic field in the anode (variation of current I_9 from I_9 =-1 A up to 0.2 A) 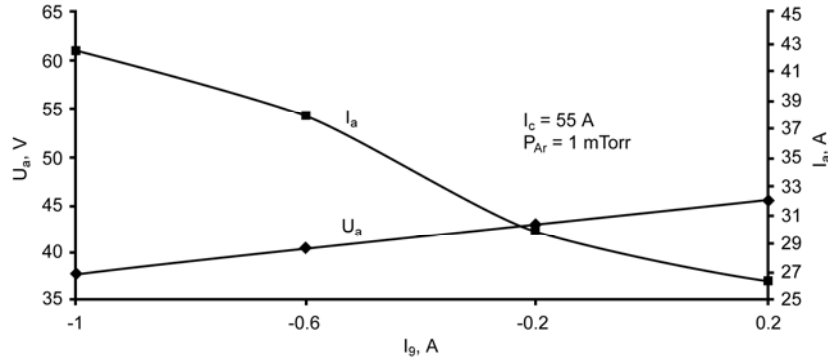causes increase in the arc voltage drop from 37 V up to 45 V. It is possible to explain such relationship as a result of increase in intensity of a longitudinal magnetic field inside the anode that makes arc current flow from the cathode to anode across magnetic field lines to be more difficult. Similar dependences are obtained for various Ar pressure. For example, decrease of Ar pressure from 2 up to 0.4 mTorr at I_9 =-1 A causes the arc voltage drop increase from 39 V up to 58 V.

4.2. Research on the arc stability at deposition of non-conducting AlN coatings (SBR supply)

The experiments show that at Ar pressure of $3 \cdot 10^{-3}$ Torr the arc burns stably, the arc voltage drop is of about 35 V. At deposition of non-conducting AlN coatings $Ar+N_2$ mix is used as the working gas. Increase in nitrogen concentration in the working mix results in the arc discharge instability that is expressed in spontaneous arc extinction. Fig. 10 (a,b) shows dependence of the arc voltage drop U_a, the anode current I_a, and also the frequency of the arc extinction **f** on Ar concentration C_{Ar} in $Ar+N_2$ mix for various current values I_9 in the anode coil 9 and fixed arc current I_c =55 A.

Fig. 11 (a,b) shows similar dependence for the arc current I_c =90 A.

The adduced dependence show, that the arc extinction is observed at $C_{Ar} < 53$ % for $I_c = 55$ A in an investigated range of current I_9 variation.

At an arc current $I_c = 90$ A stability of the arc discharge increases; arc extinction is observed at $C_{Ar} < 20$ %. Exception is the case of $I_9 = 0.2$ A, corresponding to endpoint value of the investigated range of a magnetic field in the anode, at which stability of the arc discharge is broken at $C_{Ar} \leq 33$ %.

From these data it is obvious, that deterioration of stability of the arc takes place when the arc voltage drop U_a becomes higher than $40 \div 45$ V in an investigated range of a magnetic field variations at the arc current of 55 A.

For the arc current 90 A deterioration of the arc stability occurs at greater values of U_a, i.e. when $U_a = (50 \div 55)$ V.

Deterioration of stability of the arc burning at small Ar concentration is apparently connected with formation of non-conducting AlN coating on the anode surface, resulting in

14

decrease of anode current I_a and simultaneous increase in arc voltage drop U_a. It should be noted, that the total pressure P_{Ar+N2} was varied within the range of $(2.8 \div 3.2) \cdot 10^{-3}$ Torr at the experiments. The pressure variation was, probably, the main reason of the scattering of the critical value of U_a, which accompanied the arc unstable burning in $Ar+N_2$ mix.

a)

b)
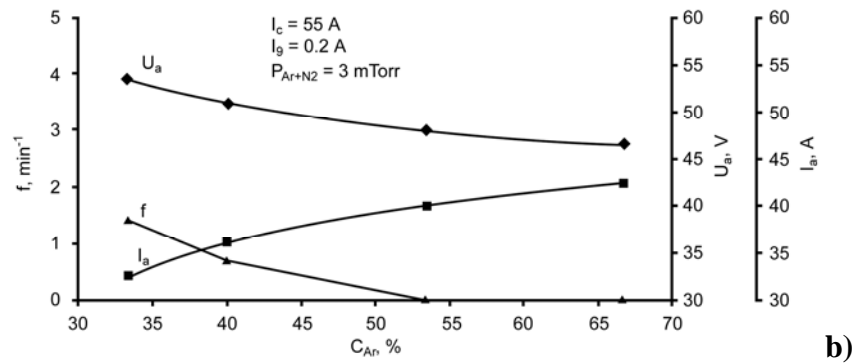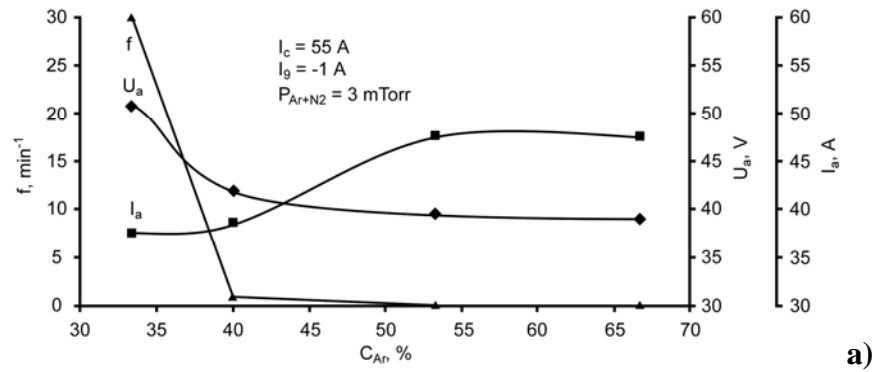
Fig.10. Arc voltage drop U_a, anode current I_a and frequency of the arc extinction **f** versus Ar concentration C_{Ar}. I_c =55 A.

a)
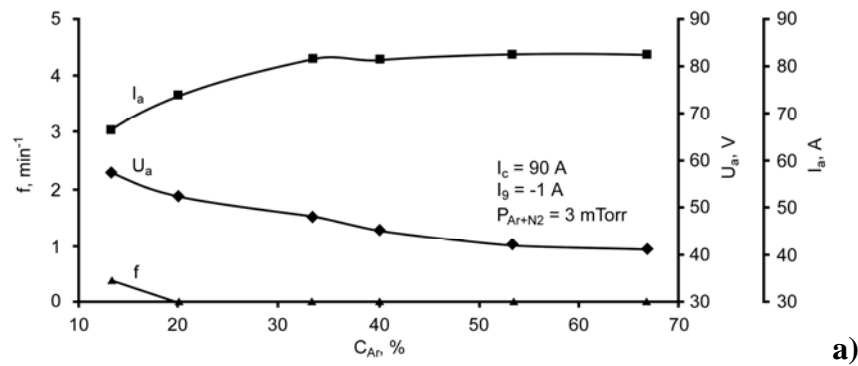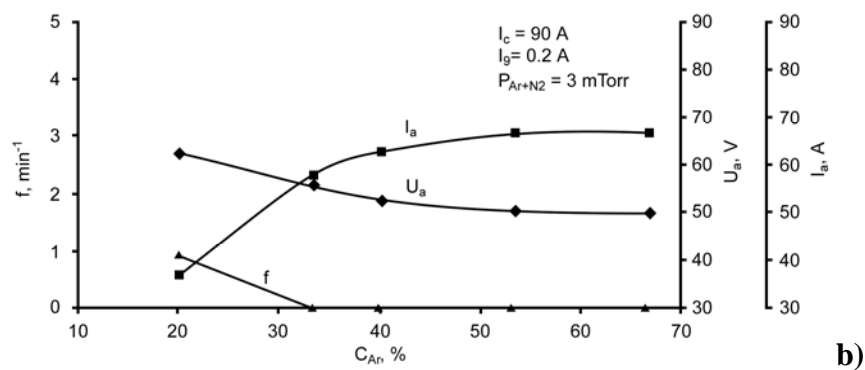
Fig.11. Arc voltage drop U_a, anode current I_a and frequency of arc breaking **f** versus Ar concentration. $I_c = 90$ A.

4.3 Description of the construction of the experimental variant of the SPS

Sketch of the experimental version of the SPS is shown in Fig. 12. Appearance of some modules of the SPS is shown in Figs.13-14. Front and rear panels of the SPS are shown in Figs.15 and 16 accordingly.

c)
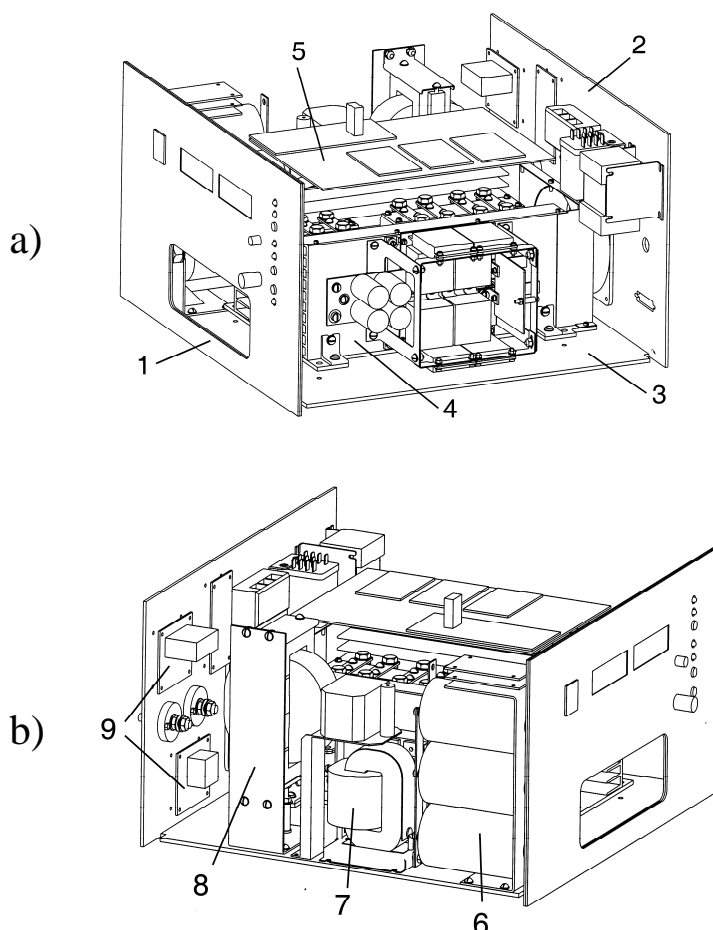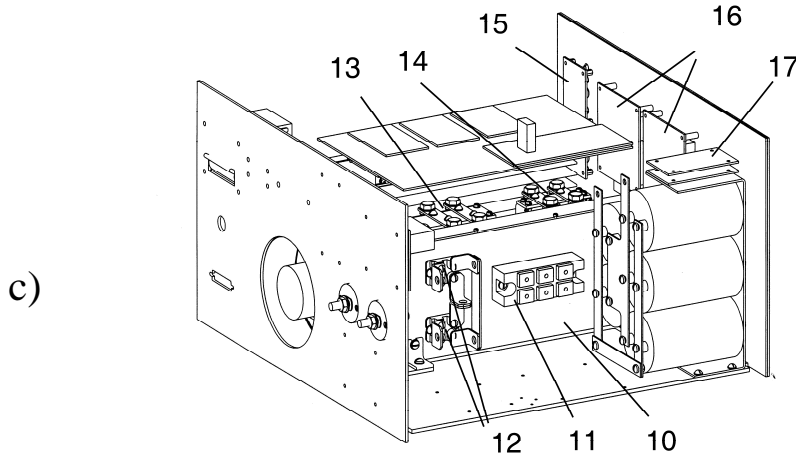
Fig. 12. Sketch of the experimental version of the SPS (without the case).

1- front panel; 2 – rear panel; 3 – bottom panel; 4 – air-cooling radiator with the IGBT power transistors; 5 – main plate; 6 – capacitors of the power supply filter; 7 – AC 50 Hz network inductor; 8 – output inductor; 9 – plates of the voltage and current sensors; 10 – air-cooling radiator for cooling the rectifier diodes; 11 – AC network rectifier; 12 – output voltage rectifier diodes; 13 – transformer; 14 – current-limiting inductor; 15 – control plate; 16 – voltage and current display plate; 17 – plate of measuring the voltage on the capacitors of the power supply filter.
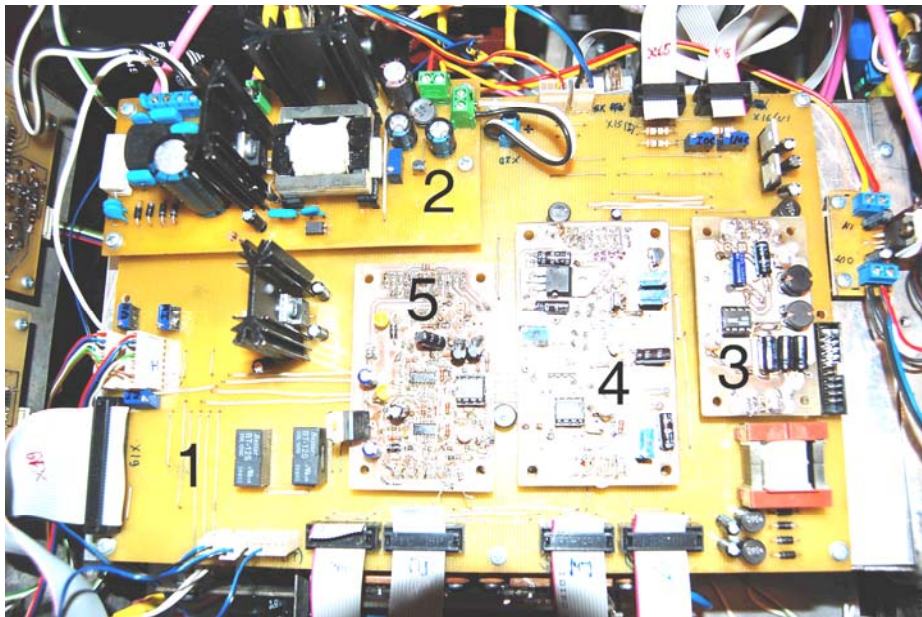
Fig. 13. Appearance of the control modules.

1 – main plate; 2 – plate of the service power supply module; 3 – plate of the generator of "meander"-shaped voltage; 4 – plate of the pulse-width modulation (PWM) regulator module; 5 – plate of automatics.
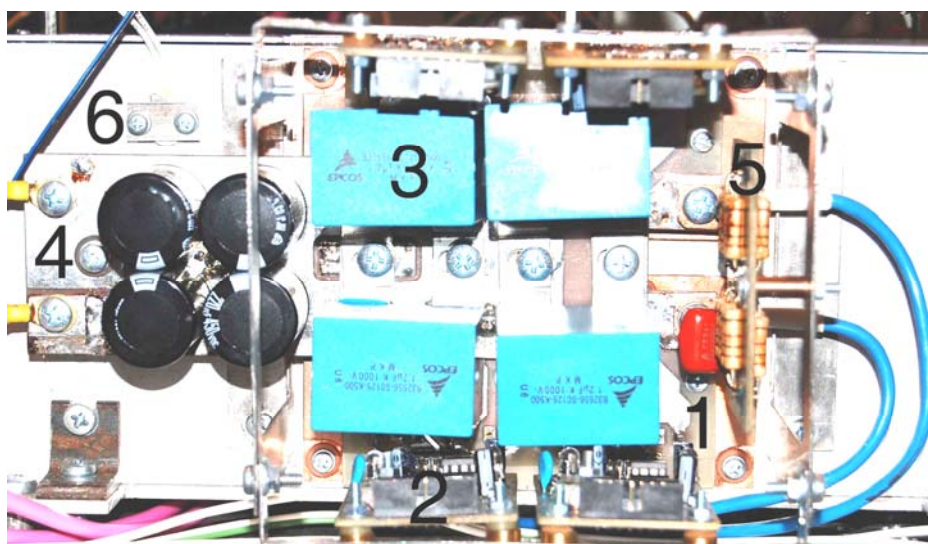
Fig. 14. Module of the bridge inverter with the IGBT transistors.

1 – plate of the IGBT transistors; 2 – driver; 3 – snubber capacitor; 4, 5 – snubber plates; 6 – thermal relay.

Fig. 15. Appearance of the front panel of the experimental version of the SPS.

1 – "On-off" switch; 2 – voltage and current displays; 3 – the output current "pre-set/measurement" button; 4 – variable resistor for regulation of an output current; 5 – control buttons ("START", "STOP" and "RESET"), 6 - indicating LEDs.

Fig. 16. Appearance of the rear panel of the experimental version of the SPS.

1 – automatic circuit-breaker; 2 – three-phase four-wire cable; 3 – interface connector of remote control, 4 – electric fan; 5 – output clamps.

4.4 Check and tuning the SPS.

4.4.1 Check and tuning the SPS modules and plates.

The unit of service power supply includes module of service power supply (see Fig. 13 pos.2), the generator of a "meander"-shaped voltage (see Fig. 13 pos.3) and other elements (pulse transformers, rectifiers and voltage stabilizers) disposed on the driver plates and current and voltage sensors plates.

Check and tuning were done in the following way:

- Tuning the service power supply plate. The plate alone was supplied with AC 50 Hz network voltage of 50-220 V. At the beginning of testing the power supply voltage was limited by the load-limiting resistor at the level of 50 V. Output voltage on contacts of the power chip was monitored by the oscilloscope. Output voltage of the service power supply plate was registered by the voltmeter. At the end of testing the power supply voltage was increased to 220 V, and load-limiting resistor was shunted. Output voltage of the service power supply was tuned to 15 V, load current was tuned to 2.5 A.

- Tuning the "meander"-shaped voltage plate. DC 15 V voltage power supply was used during tuning the plate. Clock rate of the control chip was set at 60 kHz. Overload protection of the "meander"-shaped voltage plate was tuned to operation threshold of 1 A.

- Check and tuning the overall supply plates as an assembly. During check and tuning the service power supply plate was supplied with AC voltage 220 V 50 Hz (see Fig.13 pos.2). Output

voltage of the supplies was checked by the voltmeter, and that of the "meander"-shaped voltage plate by the oscilloscope.

4.4.2. Check and tuning the system of automatics.

System of automatics is intended for realization the algorithm of SPS switching on, switching off and emergency shutdown. It consists of the circuit plate of automatics (Fig.13 pos.5), control plate (Fig.12c pos.15), the charging resistor and the relay of shunting the charging resistor. Check and tuning was carried out at de-energized AC network rectifier. Execution algorithm was checked on operation of relay of shunting the charging resistor and onset the output voltage of circuit plate of automatics which permits PWM regulator module and so the SPS operation.

4.4.3. Check and tuning the protection circuit.

Protection circuit is intended for switching-off the SPS in emergency condition. It consists of:
- current transformer plate intended for the scheme protection in case of crossing the threshold of permissible value of the current in primary winding of the pulse transformer;
- voltmeter for measuring voltage on capacitors of the network rectifier with the filter (NRF) module for protection the scheme in case of inadmissible fluctuation of the AC network voltage;
- thermal relay for protection the powerful transistors and diodes against overheating;
- scheme, disposed on the plate of drivers, intended for switching-off the SPS in case of failure the powerful transistors.

Tuning the protection schemes and voltmeter plate for measuring voltage on capacitors of the NRF module was carried out under supplying the network rectifier of the SPS with single-phase AC voltage. The voltage was varied from 30 V to 220 V. Check the current protection scheme was carried out at decreased level of output power, namely 1 kW.

Protection scheme was tuned to the operation below the threshold value (270 V) of the voltage on capacitors of the NRF module.

Simulation of the protection scheme operation in case of overheating was checked by disconnecting the thermo relay circuit.

Failure of the powerful transistor was simulated by disconnecting the circuit collector-emitter at de-energized AC network rectifier.

4.4.4. Tuning the elements of the voltage and current feedback coupling.

The elements of the feedback coupling include: the plate of the PWM regulator, the plates of the current-sensing and voltage-sensing devices and amplifiers of the sensing signals disposed at the main plate.

Tuning was carried out through two stages:
a) The first was done at de-energized AC network rectifier:
- Tuning the synchronizing clock of the PWM regulator to 25 kHz frequency.
- Check the PWM regulator with the feedback. The voltage and current feedback coupling signals were simulated by the voltage of separate supply. The output PWM regulator pulses were registered by the oscilloscope.
b) The second was done at energized AC network rectifier and with resistive load at reduced output power of the SPS (about 1 kW).

Tuning the current feedback coupling elements was done in the following way. Set-pointed reference voltage proportionate to pre-set current value was varied by the variable resistor 4 (see. Fig.15). The voltage came from the main plate and was applied to input of the amplifier of the current "mistake" disposed on the plate of PWM regulator. Signal from the sensor of the SPS output current was tuned so to bring pre-set current value in correspondence with output one.

Tuning the voltage feedback coupling elements was done in the same way, with the difference that the reference voltage was not varied and corresponded to output voltage value of 150 V.

4.4.5. Tuning the schemes of voltage and current indication.

The schemes of voltage and current indication are the digital voltmeters with upper input value of 2 V. This value should corresponds to readings of 200 V for voltmeter and 200 A for amperemeter. Signals from the current-sensing and voltage-sensing devices are amplified. Scaling schemes include amplifiers and voltage dividers. Tuning the current and voltage displays readings was carried out by using as norm the readings of standard amperemeter and voltmeter, connected to the output of the SPS.

4.4.6. Check the powerful circuits of the SPS.

The network rectifier of the SPS was supplied with single-phase AC voltage. The voltage was varied from 30 V to 220 V. Oscilloscope was used for recording the waveforms of the voltage pulses on the collector-emitter contacts of the power transistors and the current pulses on the plate of the current transformer. Output voltage and current of the SPS were monitored too. The measurements were carried out at no-load operation and under resistive load.

4.5 Test the experimental version of the SPS.

The SPS connection to three-phase 380 V 50 Hz AC network during the test is realized according to the scheme Fig. 17.
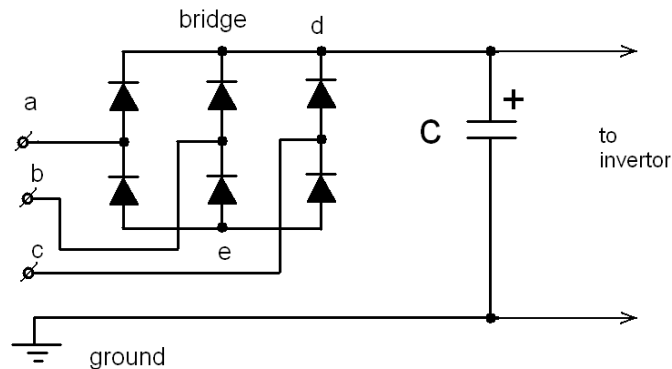

Fig.17. SPS connection to three-phase 380 V 50 Hz AC network (a,b,c – phase wires).

The phase wires are connected to the clamps a, b, c of the network rectifier (see Fig. 12c – 11). Clamp d is connected to the "+" terminal lead of the network filter capacitor C (see Fig. 12b – 6), and "-" terminal lead of the C is grounded.

Powerful variable resistor was used as the load of the SPS. The synchronizing clock rate of the PWM regulator was set at 25 kHz. Pre-set value of the output current (set with the variable resistor 4, Fig.15) was chosen at the level of 110 A.

Load characteristics of the SPS are shown in Fig. 18. Points on the plot correspond to the values of the load resistor in the range from 0.3 Ohm to 3.3 Ohm.
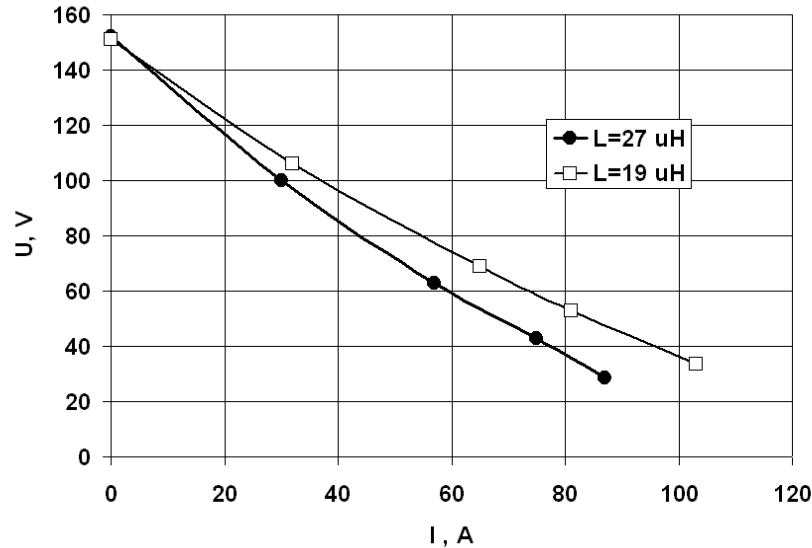
Fig. 18. Load volt-ampere characteristics of the SPS. Inductance of the current-limiting inductor is 27 µH (-●-) and 19 µH (-   -).

Apparently from Fig.18, volt-ampere characteristic is nearly linear. Earlier (see Fig.5) the SPS load V-A characteristic was calculated on the first harmonic of working frequency. Difference in shapes of calculated and measured characteristic can be explained by two reasons.

The computation was carried out in the assumption of sinusoidal form of the working frequency (only first harmonic was taken in account).

Equivalent circuit was supposed to be "ideal": voltage loss in the wires and power semiconductor elements, non-linearity of the transformer, spurious capacitance and inductance were not taken into account.

Peak power achieved was of 4.5 kW at working frequency of 25 kHz and inductance of the current-limiting inductor of 19 µH.

The tests of the experimental version of the SPS revealed emergency switching off the SPS at loaded power over 4 kW and current above 100 A after 5-10 minute of operation. The reason was inadequate cooling of the bridge circuit of the rectifier diodes (see Fig.12c pos.10) and switching off the SPS as a result of the operation of the thermal relay.
This defect was eliminated by improving rectifier diodes cooling (using more powerful fan and improving design of cooling system).

4.6   Research on stability of the vacuum arc plasma source supplied with the SPS at deposition of conductive Al coatings

The measurements were carried out according to the follow scheme. Pre-set value of the output current (set with the variable resistor 4, see Fig.15) was chosen at the level of 55 A or 90 A. The pressure of Ar was set at P=2·10^{-3} Torr and then the vacuum arc was ignited. Next the pressure was decreasing stepwise up to the moment of arc breaking. At fixed Ar pressure the values of the arc voltage drop U_a and the anode current I_a were measured. Fig. 19 (a,b) presents the dependence of the arc voltage drop U_a and the anode current I_a on pressure of gas (argon) for the fixed arc current value of I_c = 90 A at two values of current in coil 9 (I_9 = -1 A and 0.2 A).
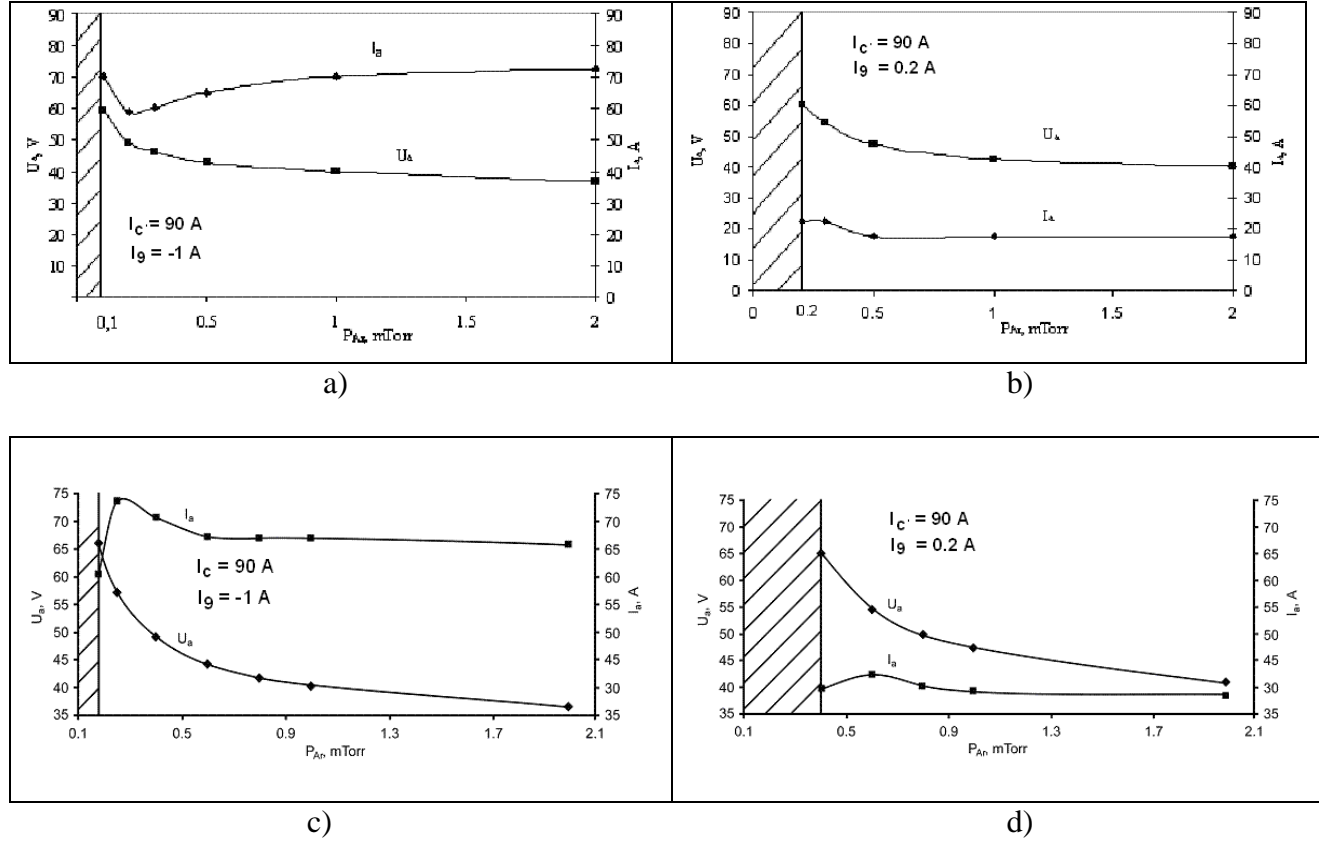
Fig.19. Dependence of the arc voltage drop U_a and the anode current I_a on working gas (argon) pressure at deposition of conductive Al coatings. Vacuum arc plasma source is supplied with SPS (a,b), with SBR (c,d).

Points in the plots of Fig.19 are placed in the pressure region of stable arc burning. Crosshatched region in the plots shows the pressure range in which the arc is broken and can't be ignited. Apparently from Fig.19 the shapes of the curves in the plots are similar for supplying the plasma source both with the SPS and SBR. However the plasma source can operate at lower pressure values when supplying with the SPS than the SBR (compare Fig.19b and 19d). In case the magnetic field strength in the anode is low (I_9= -1 A) difference in minimal pressure values at which the arc burns stably is not great (Fig.19a and 19c).

The smaller pressure, the greater arc voltage drop U_a, the more intensive regime of supply operation is, nearly the ultimate power. The data obtained confirm efficiency of the SPS developed when operated in ultimate regimes.

4.7 Research on stability of the vacuum arc plasma source supplied with the SPS at deposition of non-conductive AlN coatings

As it was noted earlier, for deposition of dielectric AlN coatings $Ar+N_2$ mix was used as the working gas and the pressure of the mix was $P_{Ar+N2} \approx 3 \cdot 10^{-3}$ Torr. The experiments carried out during the 1st Quarter have shown, that at Ar pressure of $3 \cdot 10^{-3}$ Torr the arc burns stably, the arc voltage drop is about 35 V. Addition of nitrogen in a working mix results in the arc discharge instability that is expressed in casual arc breaking. In Fig. 20 (a,b) the dependence of the arc voltage drop U_a, the anode current I_a, and also the frequency of arc breaking **f** on Ar concentration in $Ar+N_2$ mix are presented for various currents in the anode coil I_9 and fixed arc current $I_c = 90$ A.

a)   b)


c)   d)
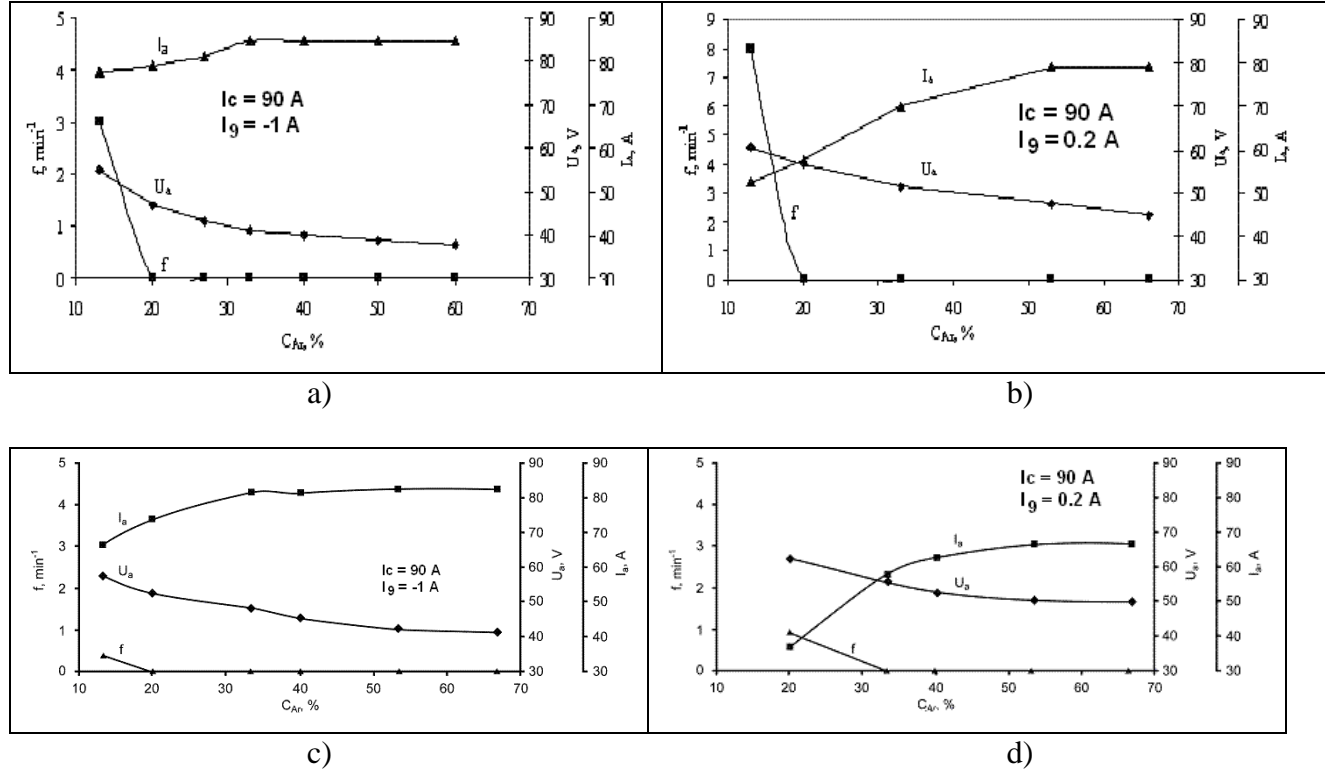
Fig.20. Dependence of the arc voltage drop U_a, the anode current I_a and arc breaking frequency f on Ar concentration in $Ar+N_2$ mix at deposition of non-conductive AlN coatings. Vacuum arc plasma source is supplied with SPS (a,b), with SBR (c,d).

For comparison in Fig.20c and 20d similar curves are presented measured with SBR supply. Comparing Fig.20a and 20c one can see that arc breaking takes place at $C_{Ar} < 20\%$ both with SPS and SBR supplies. (The dependence is obtained in the same mode of arc operation: $I_c=90$ A, magnetic field strength in the anode is determined by the value of $I_9= -1$ A). So at low magnetic field and favourable conditions for arc burning both SBR and SPS supply assures stable operation of the vacuum arc plasma source at Ar concentration in $Ar+N_2$ mix more than 20 %.

At higher magnetic field (the current value in coil 9 is $I_9= 0.2$ A), when the arc burning is hindered, SPS assures stable operation of the vacuum arc plasma source at Ar concentration in

24

Ar+N_2 mix more than 20 %, whereas SBR does it at more than 33% Ar concentration (compare Fig.20b and 20d).

From the dependence presented it is obvious that deterioration of arc stability at the arc current I_c=90A occurs when the arc voltage drop becomes greater than 45-50 V.

Observable in experiments deterioration of an arc burning stability at small Ar concentration in mix Ar+N_2 is apparently connected with formation of non-conductive AlN coating on the surface of the anode, resulting in increase of the anode – cathode electrical resistance, decrease of the anode current I_a and simultaneous increase in the arc voltage drop U_a. High value of the open circuit voltage of the SPS assures more stable operation of the vacuum arc plasma source in hindered regimes of arc burning.

It is necessary to note, that total pressure P_{Ar+N2} was varied within the range of (2.8 - 3.2) $\cdot 10^{-3}$ Torr at carrying out the experiments. The pressure variation was probably the main reason of data scattering of the value U_a, at which the arc breaking was happened in Ar+N_2 mix.

4.8 Performance of the SPS loaded with the vacuum arc plasma source

Earlier (See **4.5**) the characteristics of the SPS loaded with the active resistor were measured. Now the characteristics of the SPS loaded with the vacuum arc plasma source were measured at different regimes of operation. Investigations revealed that the electrical power transferred by the SPS in the arc discharge is varied in the range of 2-5 kW depending on working gas pressure and pre-set value of the arc current. Dependence of the electrical energy transferred by the SPS in the arc discharge on argon pressure at pre-set current value of 90 A is presented in Fig. 21.
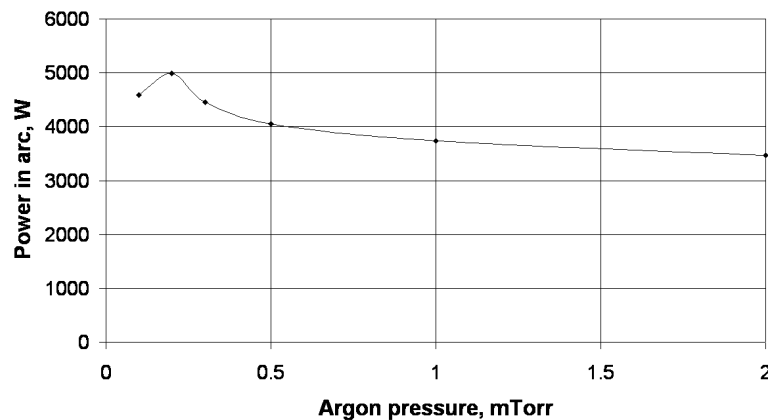
Fig.21. Dependence of the power transferred by the SPS in the arc discharge on argon pressure at pre-set current value of 90 A.

Power W was calculated on measured values of the arc current (cathode current Ic) and arc voltage drop Ua : W=Ic·Ua.

Stability of the arc current keeping is illustrated by Fig.22.
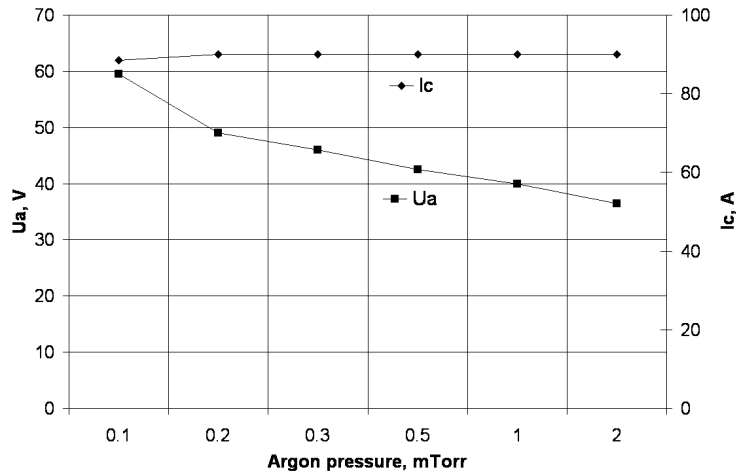
Fig.22. Dependence of the arc current (cathode current Ic) and arc voltage drop Ua on argon pressure at pre-set current value of 90 A.

From Fig.22 it is obviously that the SPS stabilize the arc current at the pre-set value of 90 A at overall range of pressure investigated, except the lowest values. At pressure value of 0.1 mTorr when the arc voltage drop is increased and power transferred by the SPS in the arc discharge is approached to ultimate level of 6 kW, minor alteration of the arc current takes place.

4.9 Characterization of the final version of the SPS

4.9.1 The main differences between the experimental and final versions of the SPS.

a)

b)

c)
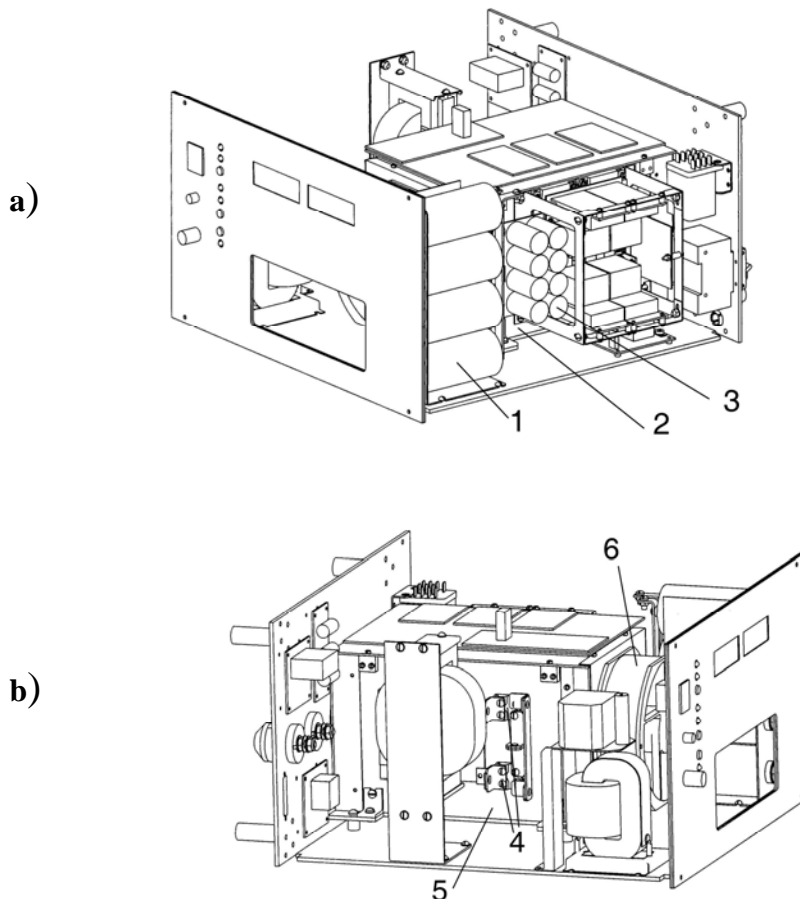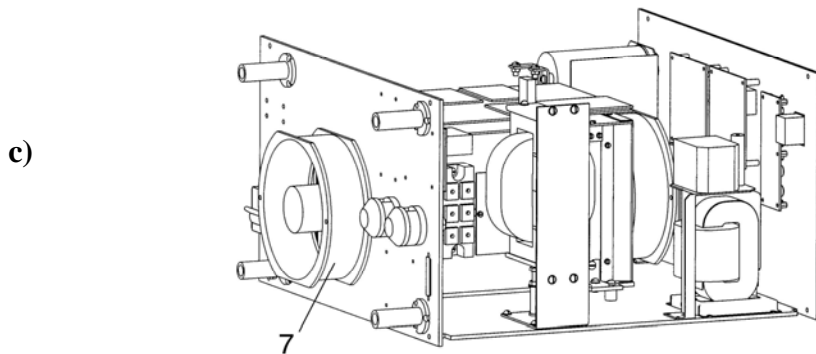
Fig.23. Sketch of the final version of the SPS.
1- capacitors of the power supply filter; 2 – air-cooling radiator with the IGBT power transistors; 3 – snubber capacitors; 4 – output voltage rectifier diodes; 5 – air-cooling radiator for cooling the rectifier diodes; 6,7 – air-cooling fans.

The tests of the experimental version of the SPS revealed insufficient cooling of the power semiconductor devices (transistors of the bridge inverted rectifier and diodes of the output rectifier).

For eliminating this deficiency and decreasing the temperature of semiconductor load-bearing elements the following actions has been made in final version of the SPS:
- air flow rate through the radiators 2, 5 was increased. The ventilating fan with productivity of 200 m^3/h was replaced by two ventilating fans 6 and 7 (see Fig. 23) of 300 m^3/h each;
- the width of radiators 2 and 5 was increased from 120 mm up to 165 mm;
- for more efficiency of power diodes cooling they have been replaced at the edge of a radiator, near to the input of cooling air flow.

Besides during trials of the experimental version of the SPS the temperature of the snubber capacitors 3 (see Fig. 23) was increasing up to 50 ºC. The possible reason was high level of current pulsations. When capacity of the snubbers was increased from 1.2 up to 1.6 mF their temperature did not exceed 40 ºC.

For minimizing the inductance of the connecting wires, the capacitor bank of the supply-line filter 1 has been located more close to snubber capacitors 3 that also allowed reduce the level of pulsations.

Tests of the experimental variant of the SPS with the vacuum-arc plasma source have shown, that the amplitude of the surge voltage pulses on the diodes of a rectifier diode bridge can reach 300 V (see Fig. 24), at a peak voltage permissible for these diodes of 400 V.
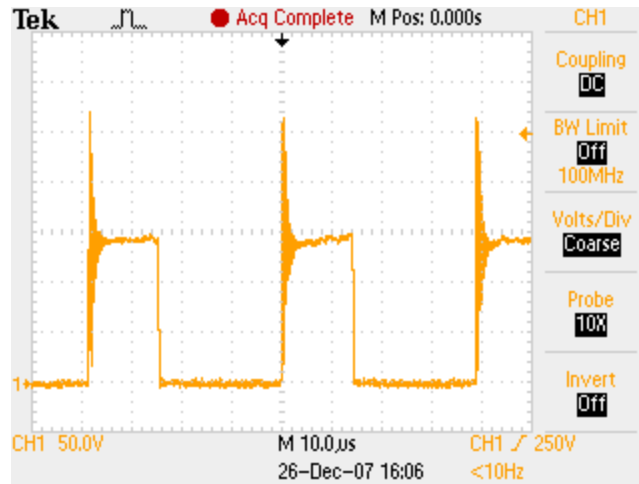
Fig. 24. Waveform of the voltage on the rectifier diodes when the SPS is loaded with the vacuum-arc plasma source.

For smoothing these pulses the capacitance of the snubber capacitors have been increased from 0.01 μF up to 0.1 μF. It has allowed reduce the amplitude of the pulses on 20-30 V (i.e. on 30 % from the initial value).

4.9.2 Adjustment and trial of the final version of the SPS loaded with the active resistor (BR).
The adjustment procedure was the same as reported earlier in **4.4.**
Resulting voltage-current characteristics for synchronizing clock rate f of the PWM regulator of 25, 30 and 32 kHz are presented in Fig. 25.
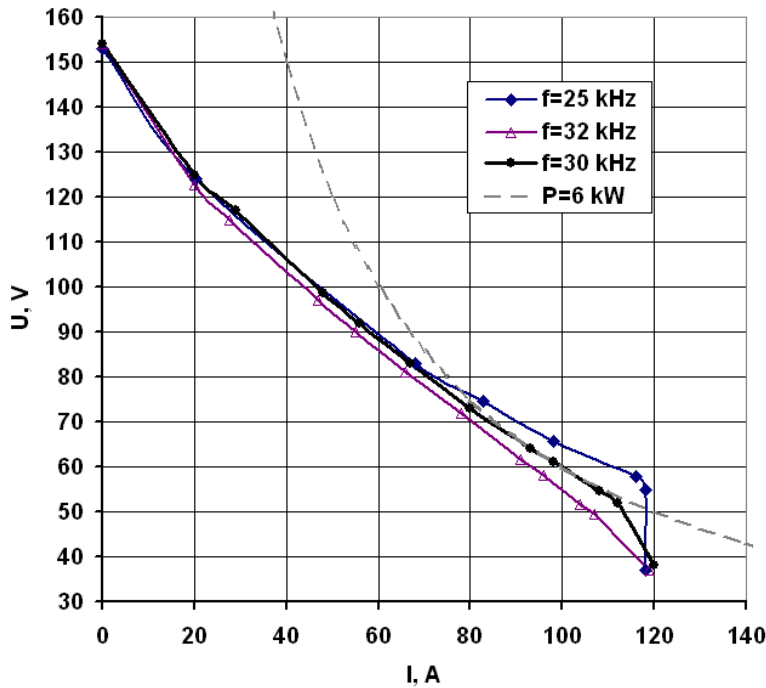
Fig.25. Load volt-ampere characteristics of the final version of the SPS. The synchronizing clock rate f of the PWM regulator is 25 kHz, 30 kHz and 32 kHz. Dashed-line is the curve of constant power (P=6 kW).

Apparently from the voltage-current characteristics in Fig.25 the optimum value of the synchronizing clock rate f of the PWM regulator is 30 kHz. Such performance ensures the operation the SPS within the limits of a permissible power (up to 6 kW). At frequency f=25 kHz the output power can attain 6.5 kW and call an overload of the power supply. The SPS voltage-current characteristic for f=32 kHz is situated below the curve of constant power (of 6 kW). In this case a voltage drop on a ballast inductor restricts the output power of the SPS at the level of 5.5 kW.

During trials temperature of the housing of the load-bearing elements (power transistors and the output rectifier diodes) were measured. Measurements were carried out at the peak SPS parameters: output current of 120 A and power of 6 kW. The temperature of these devices did not exceed 50 ºC. The temperature of the snubber capacitors did not exceed 40 ºC.

4.9.3 Performance of the final version of the SPS loaded with the vacuum arc plasma source.

The characteristics of the final version of the SPS loaded with the vacuum arc plasma source were measured at different regimes of operation. The electrical power transferred by the SPS in the arc discharge was varied in the range of 3-5 kW depending on working gas pressure and pre-set value of the arc current. Dependence of the electrical energy transferred by the final version of the SPS in the arc discharge on argon pressure at pre-set current value of 90 A and 120 A is presented in Fig. 26.
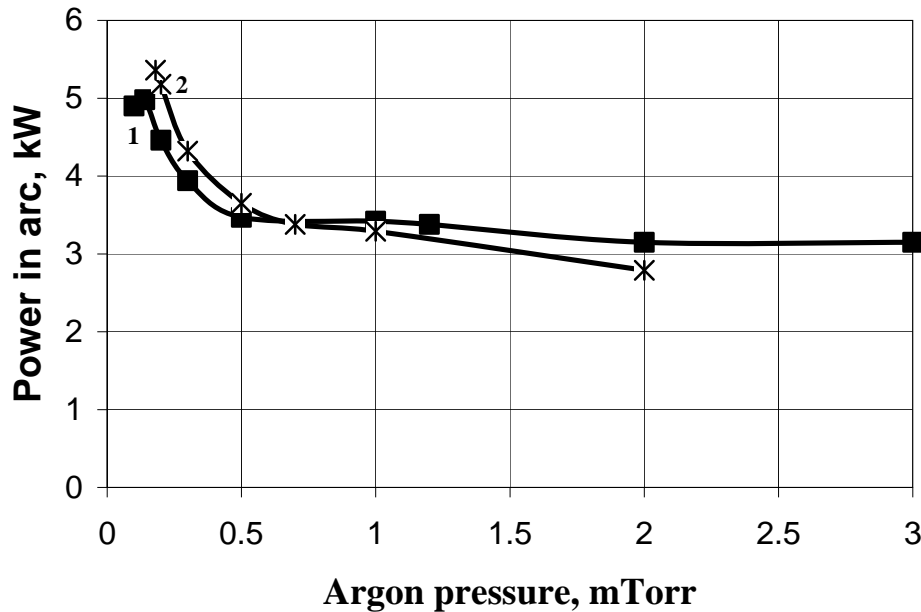

Fig.26. Dependence of the power transferred by the final version of the SPS in the arc discharge on argon pressure at pre-set current value of 90 A (1) and 120 A (2).

Power W was calculated on measured values of the arc current (cathode current Ic) and arc voltage drop Ua : W=Ic·Ua.

According to the Work Schedule the final version of the SPS was tested when operating with the vacuum-arc plasma source under dielectric coating deposition. Research on stability of the vacuum arc plasma source supplied with the final version of the SPS was carried out at deposition of non-conductive AlN coatings. $Ar+N_2$ mix was used as the working gas and the pressure of a mix was $P_{Ar+N2} \approx 3 \cdot 10^{-3}$ Torr. Stability of the vacuum arc plasma source operation was found to be the same as in case of supplying with the experimental variant of the SPS (see **4.7**).

5. Conclusions

Research on stability of a filtered vacuum-arc plasma source operation with Al cathode provided with the standard power supply with a ballast resistor (SBR) has been carried out at deposition of both conducting metal and non-conducting dielectric coatings.

It has been shown, that at deposition of conducting Al coatings the plasma source operates stably at pressure $P_{Ar} \geq 0.3 \cdot 10^{-3}$ Torr (I_c =55 A) and at $P_{Ar} \geq 0.4 \cdot 10^{-3}$ Torr (I_c =90 A) in an investigated range of magnitudes of the magnetic field inside the anode. Thus the maximal value of the arc voltage drop U_a changed in range (52 ÷ 68) V at I_c =55 A. and U_a = (49 ÷ 65) V at I_c =90 A. At P_{Ar}=2·10^{-3} Torr the arc voltage drop U_a decreased down to U_a = (35.5 ÷ 39.5) V.

Influence of the magnetic field inside the anode on stability of the vacuum-arc plasma source operation was investigated. At variation of current in the coil 9 (and accordingly the magnetic field inside the anode) within the limits of I_9 = (-1 ÷ 0.2) A the arc voltage drop U_a at the arc current I_c of 55 A and pressure P_{Ar}=0.4· 10^{-3} Torr varied in range of U_a = (46 ÷ 65) V. At the arc current of 90 A and variation of the current in the coil 9 within the limits of I_9 = (-1 ÷ 0.2) A the range of the arc voltage drop was U_a = (50÷65) V for P_{Ar}=0.4·10^{-3} Torr, and U_a = (37÷43) V for P_{Ar}=2·10^{-3} Torr.

Research on stability of the source operation in various modes at synthesis dielectric AlN coatings were carried out.

It was shown, that at total pressure of $Ar+N_2$ mix P_{Ar+N2}=3·10^{-3} Torr stability of burning of an arc depends both on Ar percentage in the mix, and on arc current I_c. In particular it was shown, that at I_c =55 A the arc is stable, if Ar concentration in $Ar+N_2$ mix is greater than C_{Ar}= 53 % in a range of (-1 A ÷ 0.2 A) variations of a current in coil I_9. At the arc current of 90 A the arc stability was provided at lower Ar concentration in the mix: $C_{Ar} \geq 20$ % at I_9 = (-1 ÷ -0.6) A and $C_{Ar} \geq 33$ % at I_9 = (-0.2 ÷ 0.2) A.

The assumption was made, that deterioration of stability of an arc burning at small Ar concentration in $Ar+N_2$ mix is connected with formation of non-conducting AlN coating on a surface of the anode, resulting in decrease of the anode current I_a and simultaneous increase in the arc voltage drop U_a.

The scheme and design of the main units and the SPS as a whole was developed. The experimental version of the SPS was manufactured and tested. Peak power of 4 kW and current of 105 A was achieved in the load (active resistor of 0.3 Ohm). On the base of the data obtained debugging and modifications were made. Cooling of the rectifier diodes was increased and the current-limiting inductor with lower inductance was used to provide proper heat regime of power elements and achieve planned power of 6 kW.

The performance of the vacuum-arc plasma source supplied with the experimental version of the SPS was investigated. Vacuum-arc discharge characteristics were measured in the regimes of deposition of conductive Al and non-conductive (dielectric) AlN coatings. Stability of the vacuum-arc plasma source operation was investigated. Frequency of casual arc breaking was measured.

Comparison was made of the performance of the vacuum-arc plasma source supplied with SPS and SBR in the regimes of deposition of conductive Al and non-conductive AlN coatings. SPS was shown to provide stable vacuum arc source operation at lower Ar pressure than SBR at deposition of the conductive coatings. In the regimes of deposition of non-conductive AlN coatings the arc with SPS supply burns at lower Ar concentration value in Ar+N_2 mix (20% instead of 33% with SBR supply), that is at highest concentration level of nitrogen in the working mix.

The value of the electrical power transferred by the SPS in the arc discharge was measured in various modes of the source operation. It was demonstrated that the power value was varied in the range of 2-5 kW depending on the working gas pressure.

Stability of keeping the pre-set value of the arc current was explored. It was clarified that the SPS keeps up the pre-set current value with high accuracy. Only minor alteration of the arc current takes place at pressure value of 0.1 mTorr when the arc voltage drop is increased and power transferred by the SPS in the arc discharge is approached to ultimate level of 6 kW.

Final version of the PSS was manufactured and tested.

Trials of the final version of the SPS loaded with BR have shown that modernization of the experimental version of the SPS permitted:
- considerably reduce temperature of power semiconductor devices down to 50 ˚C, and that of the snubber capacitors to 40 ˚C;
- reduce the amplitude of a surge voltage pulses on the power diodes on 20-30 V;
- attain an optimal voltage-current characteristic of the SPS.

When optimization of the design was done, then reliability of operation, planned power value of 6 kW and the upper limit output current value of 120A were reached in final version of the SPS.

6. References

1. J.M.Lafferty. *Vacuum arcs*. 1980.
2. I.M.Gottlieb. *Power supplies, switching regulators, inverters and converters*. 1994.
3. *Manual on DC power supply, DHP series*. Sorensen.

List of symbols, abbreviations and acronyms

BR - ballast resistor
SBR - power supply with ballast resistor
SPS, or PSS - switching power supply source
PWM - pulse-width modulation
PFM - pulse-frequency modulation
FVAPS - filtered vacuum-arc plasma source
I_a - anode current
I_c - arc current
I_{load} - load current
C_{Ar} - argon gas concentration in (Ar+N_2) mix

P_{Ar} - pressure of Ar
f - frequency of arc breaking
U_a - arc voltage drop
AUT - module of automatics;
DRV - drivers;
IND - module of control and indication;
INT - interface of remote control;
INV - inverter;
L_b - ballast inductor coil;
NRF - network rectifier with the filter
ORD - output rectifier with an inductor coil;
REG - PWM regulator module;
SEN - module of measuring instruments;
T - pulse transformer;
VAP - vacuum-arc plasma source.

APPENDIX. USER'S MANUAL ON SPS

A1. PURPOSE AND CAPABILITIES

A1.1 The SPS power supply is general purpose power supply designed specifically for DC vacuum-arc plasma sources.
The main features:

- transformation input AC network power into output DC power.

- measuring and displaying the output current and the output voltage on the load.

- pre-set and adjusting the output current.

- fault signalling in emergency state.

A1.2. Environmental characteristics.

Ambient temperature (operating)	of +10 °C to 40 °C.
Humidity	of 0 – 85 % RH, non-condensing.
Altitude	up to 2000 m.

Ambient should be non-dangerously explosive, without corrosion vapours and gases, without electro-conducting dust.
Horizontality of the device rack should be inside the range of 0 - 5°.

A2. TECHNICAL CHARACTERISTICS

A2.1 **Input network**.

Voltage	3 phase 220 V AC
- Deviations of the input voltage (permissible)	+10, -15%
- Frequency	50-60 Hz

A2.2 **Output circuit parameters**.

- Output current   in the range of 20-120 A
- Maximal output current   120 A
- Output current fluctuations   at the most 1 % *
- Open circuit voltage   150 V
- Output voltage at output current of 120 A   50 V *
- Output terminals are isolated from the ground.

* on the active load

A2.3 Maximal output power   at the most 6 kW

A2.4 Power factor (minimal value)   0.9

A2.5 Efficiency (minimal value)   90 %

A2.6 Switching frequency   30 kHz

A2.7 Regime of operation   long-term

A2.8 There is the display of the regimes of SPS operation

A2.9 Cooling   internal fans

A2.10 **Physical characteristics**:

Width   520 mm

Depth   485 mm

Height   270 mm

Weight   31 kg

A3. OPERATING INSTRUCTIONS

A3.1. Ensure that facility AC input power is de-energized prior to connecting or disconnecting the input/output power cabels.

A3.1.1. Connect the input power cabel to AC power network 220 V 50-60 Hz according to the Table A1.

ATTENTION! THE POWER SUPPLY OPERATION AT DISCONNECTED GROUND WIRE IS FORBIDDEN!

A3.1.2. Connect the electrodes of the vacuum-arc plasma source to the terminals 2 (threaded studs, see Fig.A1) keeping the polarity: the cathode to the terminal "-" and the anode to the terminal "+".

OPERATE WITH THE SAFETY GROUND!

A3.2. "**Turn on**" procedure.
A3.2.1. Energize the 220 V AC network power cable. Turn on the automatic circuit-breaker 1 on the rear panel (see Fig.A1) then turn on the circuit-breaker "POWER" on the front panel. The LED "SPS" should begin to light, the cooling fans should begin operated and zeroes ** should be appeared on the displays "CURRENT" and "VOLTAGE".

ATTENTION! The LED "Fault" can begin to light sometimes owing to transient processes in the control system. In this case push the knob "Reset", the LED "Fault" should be go out.

The SPS is ready for operation.

A3.2.2. Push and keep the knob "Setup" and adjust the desired pre-set value of the arc current by manipulating the tuning knob "Current Regulator".
A3.2.3. Push and then release the knob "Start" and wait for 2-3 sec. The LED "Force" should begin to light and the voltage value of 150 ± 5 V should be displayed at the indicator "Voltage".
A3.2.4. If the LED "Fault" began to light, push and then release the knob "Reset" and then repeat the operation on point A3.2.3.
A3.2.5. Turn on the arc ignition device
A3.2.6. The pre-set value of the arc current one may adjust during the SPS operation.
A3.2.7. If the arc current value isn't displayed on the panel "CURRENT", turn off the arc ignition device and the SPS (see point A3.3).
A3.2.8. Check the discharge gap of the vacuum-arc plasma source and the circuit "anode – cathode".
A3.2.9. Repeat the "turn on" operation according to the point A3.2.1–A3.2.6.
A3.2.10. If the fault of point A3.2.7 will be repeated, ask the SPS designer and manufacturer.

** The digits in decimal position on the right of Zero can be lighted at the panel.

A3.3. "Turn off" procedure.
A3.3.1 Turn off the ignition device.
A3.3.2 Push the knob "Stop".
A3.3.3 Over 2-3 minutes turn off the circuit-breaker "POWER". Turn off the automatic circuit-breaker, located at the rear panel.

A4. SOME CONCEVIABLE FAILURES

A4.1. During the SPS operation in case of the output current overload or output power cables failure the LED "Fault" can be light. In such situation it is necessary turn off the SPS following

the procedure of point A3.3, make sure of serviceability of the load circuit and the output power cable and then push the knob "Reset". (**NOTE** that if the knob "Stop" was not pushed during the switching off procedure execution, the SPS will turn on automatically after pushing the "Reset" knob).

A4.2. At frequent occurrence of the failure of the type of A4.1 ask the SPS designer.

A4.3. At overheating of the powerful elements of the device the LED "Overheating" begins to light. Conceviable cause may be the air fans failure or clogging of the air cooling channels. For solving this problem it is necessary check the fans serviceability and to clean the air-channel. **NOTE** that the thermo-sensor's characteristic has hysteresis in time, that's why the SPS becomes respond to the knob "Reset" only after cooling.
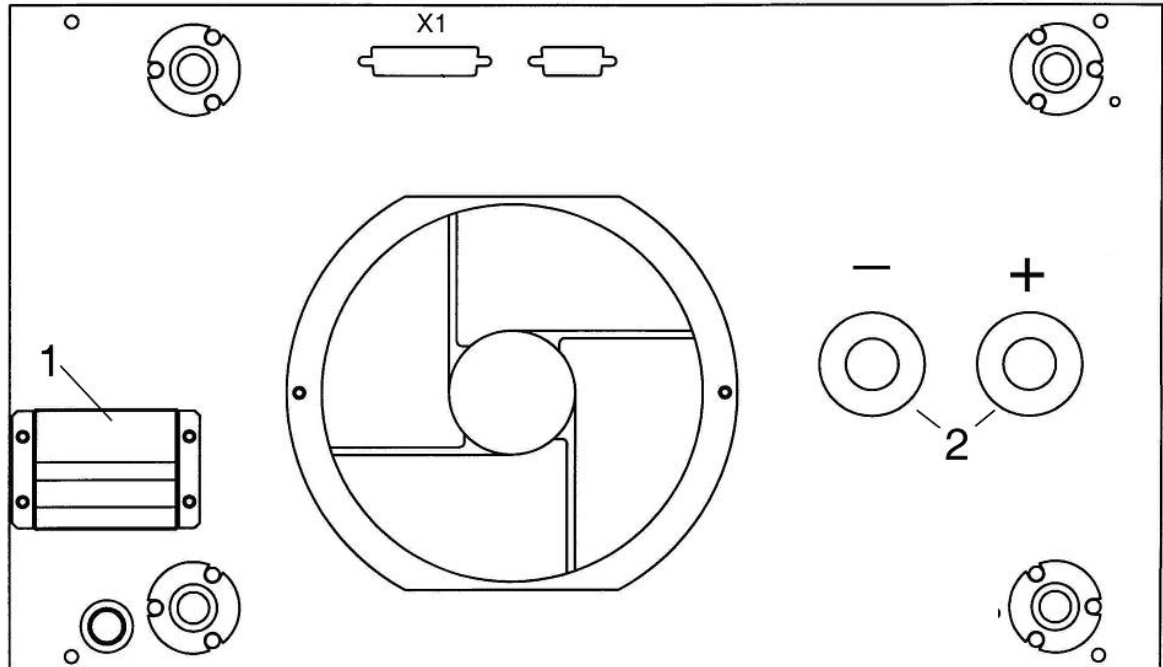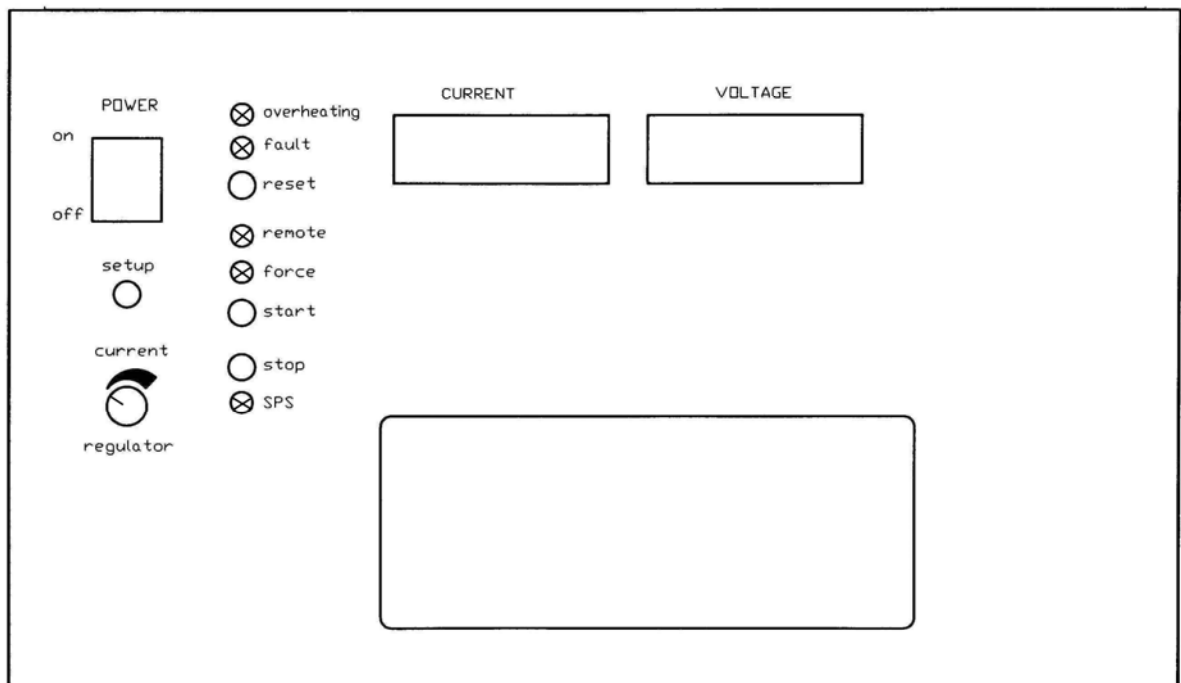
Fig.A1. Front and rear panels of the SPS.
1 – automatic circuit-breaker; 2 – output terminals (M8 threaded studs).

Table A1. Designations and color of the wires of the input AC power cable.

Ground	Phase "A"	Phase "B"	Phase "C"
Black and white	Yellow	Blue	Brown